Convection in GATE

ROBERT A. HOUZE, JR.

Department of Atmospheric Sciences, University of Washington, Seattle, Washington 98195

ALAN K. BETTS

West Pawlet, Vermont 05775

The difficult problem of parameterizing tropical convection in large-scale models of the atmosphere led to the Global Atmospheric Research Program's Atlantic Tropical Experiment (GATE), whose goal was to improve basic understanding of tropical convection and its role in the global atmospheric circulation. A dense network of instrumented ships equipped with upper air sounding equipment and quantitative weather radars were located over the Atlantic Ocean, in the intertropical convergence zone (ITCZ), just west of equatorial Africa. The ship network was supplemented by a fleet of research aircraft and a geosynchronous meteorological satellite. The data obtained show that the deep convection in the ITCZ was concentrated in two types of 'cloud clusters,' rapidly moving squall clusters, and slowly moving nonsquall clusters. The clusters were characterized by large mid-to-upper level cloud shields, or 'anvil clouds,' that emanated from penetrative cumulonimbus convection. Accompanying the deep cumulonimbus in each cluster was a log normal spectrum of smaller convective features ranging from moderate cumulonimbus down to tiny nonprecipitating cumulus. The large cumulonimbus were typically grouped within a cluster into one or more mesoscale precipitation features (or MPF's), which were apparently triggered in mesoscale regions of intensified low-level convergence. As an MPF matured it developed a region of stratiform precipitation adjacent to its active deep convective cells. The stratiform precipitation fell from the anvil cloud. Associated with the stratiform precipitation were a mesoscale downdraft below the anvil cloud and an apparent mesoscale updraft within the anvil cloud itself, above the mesoscale downdraft. These mesoscale drafts were distinct from the convective-scale updrafts and downdrafts of the cumulus and cumulonimbus cells of the cluster. Downdrafts, both convective scale and mesoscale, filled the planetary boundary layer in the vicinity of cumulonimbus with stable air of low moist static energy. These wakes of downdraft air exerted a strong control on where future convection broke out. The results of GATE show that to simulate the effects of tropical convection in large-scale numerical models of the atmosphere a variety of phenomena must be accounted for, including not only convective-scale updrafts and downdrafts but anvil clouds with mesoscale updrafts and downdrafts, downdraft-induced boundary layer transformations, and mesoscale convergence patterns. Experimentation with ways of including some of these features of tropical convection in large-scale diagnostic and prognostic studies is under way, but much work remains to be done.

CONTENTS

A. THE UNDERSTANDING OF TROPICAL CONVECTION IN 1973

While it had been recognized well before the planning of the Global Atmospheric Research Program's Atlantic Tropical Experiment (GATE) that deep convection over the equatorial oceans is a primary mechanism for transporting heat from the planetary boundary layer to the upper troposphere [*Riehl and Malkus*, 1958], it was just becoming evident during the planning of the experiment (from accumulating satellite evidence) that this convection was concentrated in 'cloud clusters' [*Martin and Karst*, 1969; *Frank*, 1970; *Martin and Suomi*, 1972]. During GATE planning meetings a cloud cluster came to be defined as a group of cumulonimbus joined in their mature and dissipating stages by a common cirrus shield ~100 to 1000 km in horizontal dimension [*International Council of Scientific Unions/World Meteorological Organization (ICSU/WMO)*, 1970]. The bright cirriform tops of the clusters were seen to dominate the satellite-observed cloud patterns over the equatorial oceans [*Kornfeld et al.*, 1967]. The clusters seen in satellite imagery appeared and disappeared somewhat sporadically [*ICSU/WMO*, 1972, p. 28]; however, *Reed and Recker* [1971] showed that cloud cluster frequency over the equatorial

Pacific Ocean was modulated by the passage of synoptic-scale waves in the easterlies.

Heat and moisture budgets in the vicinities of tropical cloud clusters were determined from rawinsonde data by several investigators in the early 1970's. *Gray* [1973] suggested that the budgets that were obtained could be explained only if an average cloud affected its large-scale environment through a combination of dry compensating subsidence, which warmed the environment, and detrainment of hydrometeors, which evaporated and thereby cooled the environment. *Yanai et al.* [1973], *Ogura and Cho* [1973], *López* [1973], and *Nitta* [1975] used one-dimensional cumulus models to show that this was the case. *Betts* [1973b] presented similar arguments in his studies of cumulonimbus clouds over Venezuela.

The approaches of *Yanai et al.* [1973], *Ogura and Cho* [1973], and *Nitta* [1975] provided a particularly useful mathematical framework for the study of convection in GATE. Their equations employing simple cumulus models to diagnose convective cloud properties from observed large-scale budgets paralleled those used by *Ooyama* [1971] and *Arakawa and Schubert* [1974] in their schemes for the parameterization of convection in numerical models of large-scale atmospheric flow. It was evident, however, that the usefulness of the results of the diagnostic techniques or parameterization schemes depended on the adequacy with which the assumed cloud models actually described the component clouds of clusters.

Questions about this adequacy were already evident in 1973. During the Line Islands experiment, aircraft and other detailed observations of one cloud cluster showed that its common cloud shield was in the form of a stratiform 'anvil' cloud trailing a line of deep cumulonimbus cells [*Zipser*, 1969]. The base of the anvil was at middle levels (4–5 km), and general nonconvective precipitation was falling from it. This widespread rain was evaporating as it fell, thereby cooling the air below the anvil cloud. The cooled air was subsiding in a general mesoscale downdraft extending over a region several hundred kilometers in horizontal scale. Similar mesoscale downdrafts were also noted by *Riehl* [1969] in oceanic cloud clusters and by *Betts* [1973b] in Venezuelan cumulonimbus.

From these observations it was apparent that mesoscale as well as cumulus-scale vertical motions could be important circulation features in cloud clusters. Such structure was considerably more complex than the mathematically simpler types of clouds assumed in diagnostic calculations or parameterization schemes.

B. THE AIMS OF GATE IN IMPROVING THE UNDERSTANDING OF TROPICAL CONVECTION

Against this background of the general understanding of tropical convection at the time of the planning of GATE, it is not surprising that the experiment was designed '. . . to provide a description of the internal structure of a number of cloud clusters, to estimate the vertical (and horizontal) transport of heat, moisture and momentum associated with the systems and to related them to movements of the tropical atmosphere on a larger-scale' [*ICSU/WMO*, 1972, p. 7]. The descriptions would be made possible by employing a variety of special observing systems. At the same time, the large-scale budgets of mass, heat, momentum, and other quantities would be determined from intensive soundings of the atmosphere in the vicinity of the convection. Diagnostic techniques of the type pioneered by *Yanai et al.* [1973], *Ogura and Cho* [1973], and *Nitta* [1975] could then be used to deduce cloud proper-

ties, and these properties could be compared with those shown directly by the special observing systems. In this way the physical understanding of tropical convection would be increased, and the adequacy of cloud models used in diagnostic studies (and parameterization schemes) would be determined. Moreover, as large-scale atmospheric conditions shown by the soundings were observed to change during the course of the experiment, for example, diurnally or with the passage of easterly waves, associated changes in the observed convective processes could be noted.

C. METHODS OF OBSERVING THE CONVECTION IN GATE

In GATE the standard approach of combining satellite, radar, aircraft, and highly resolved upper air balloon data was adopted to probe the convective cloud field. These data were supplemented by standard synoptic observations, surface-based cloud photography, and a variety of boundary layer measurements. Each type of data collected contributed in a unique way to an understanding of the cloud fields. The principal types of data are discussed below.

1. Satellite

During the summer of 1974 the geosynchronous meteorological satellite SMS 1 was positioned to provide detailed imagery over the GATE area. These data, obtained at 15- to 30-min intervals throughout the experiment, provided a detailed history of the development of cloud patterns over the GATE region. However, since the satellite data portrayed only the tops of the clouds, it was necessary to use other instrumentation to probe their internal structures.

2. Radar

The internal structures of GATE cloud systems were revealed by a network of weather radars, which showed the precipitation fields of the systems. Eight GATE ships carried radars [*Arkell and Hudlow*, 1977], of which four were C band and equipped for digital data acquisition. Characteristics of the digital radar systems, which were arranged spatially to allow overlapping coverage (Figure 1), are described by *Hudlow et al.* [1980]. Three-dimensional fields of radar reflectivity (or precipitation intensity) were recorded simultaneously by all four digital radars at 15-min intervals throughout GATE.

3. Aircraft

Although combined radar and satellite data, with the aid of surface-based cloud photography, gave a fairly complete description of the structure and evolution of the cloud and precipitation fields in GATE, these remote measurements gave no direct information (other than cloud top temperature) on the values of dynamical or thermodynamical variables within or near cloud systems. Measurements of these quantities were obtained by direct aircraft sampling of GATE cloud systems. The aircraft also provided additional cloud photography, turbulent flux measurements, radiation measurements, dropwinsondes, aerosol observations, and cloud microphysical data.

Thirteen aircraft were used in GATE to make more than 400 research flights. Many of these flights were made in the vicinity of the shipborne radar network, thus providing detailed measurements near and within the same cloud systems being observed by radar and satellite. Summaries of the various aircraft missions are presented by *Kelley* [1974] and *ICSU/WMO* [1975]. Listings of the types of measurements and ob-
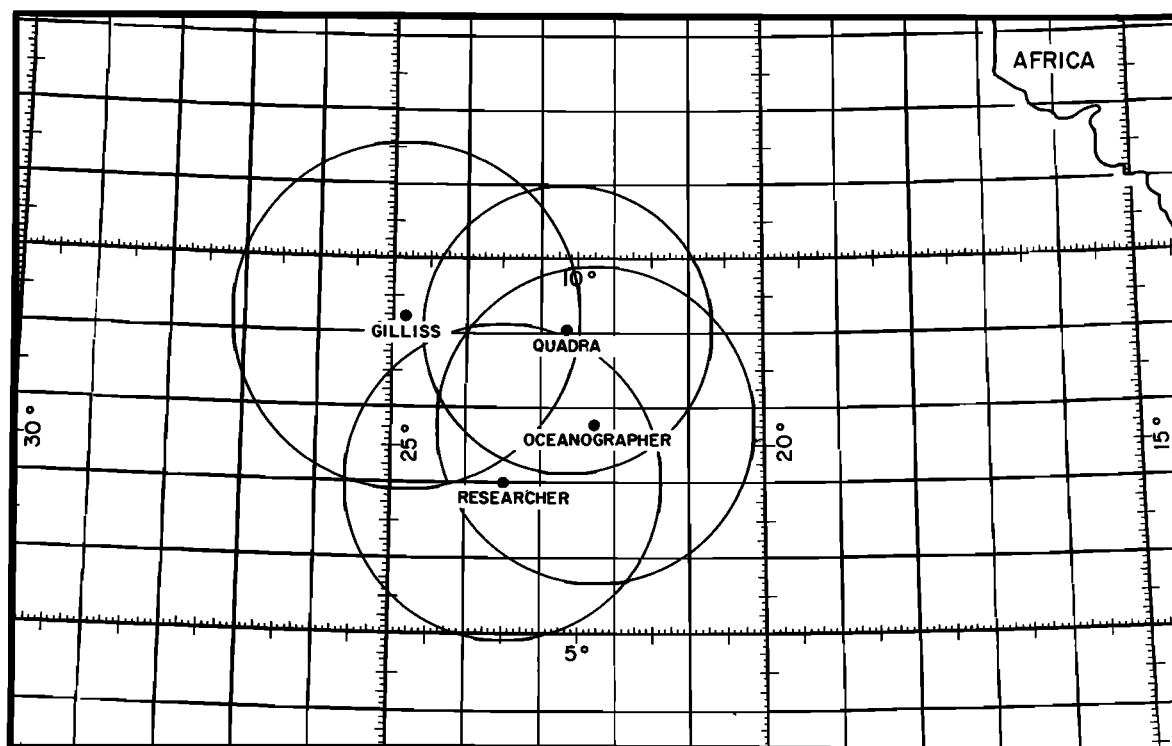
Fig. 1. Positions of ships carrying quantitative radars during Phase III of GATE (August 30 to September 10, 1974). A somewhat different arrangement was used in Phases I and II. From *Houze* [1977].

servations recorded during these flights can be found in the GATE Data Catalog (available from World Data Center-A, National Climatic Center, Asheville, North Carolina).

4. Upper Air Soundings

Upper air soundings in GATE were launched at 3-hour intervals from ships arranged within a hexagonal region surrounding the shipborne radar network. With this distribution of sounding sites it was possible to monitor the structure of the large-scale environment in the vicinity of the cloud systems being observed by satellite, radar, and aircraft.

D. STATISTICAL SURVEYS OF GATE CONVECTION

The main array of ships in GATE was located so that it would be on or near the axis of the east-west belt of cloudiness and precipitation associated with the intertropical convergence zone (ITCZ) [*ICSU/WMO*, 1972]. Thus statistical studies of the various types of data collected within or near the array would reflect the mean properties of the convection in the ITCZ during the experiment. A variety of statistical and quasi-statistical studies have now been performed, and they are summarized below.

1. The Mean Rainfall Pattern in the ITCZ

The mean rainfall patterns within the GATE ship array were determined from the shipborne weather radars and have been presented by *Hudlow* [1979] (see Figure 2). These patterns are consistent with shipboard rain gage measurements [*Hudlow et al.*, 1980] and with water vapor budgets derived from the upper air soundings obtained in the ship array [*Lord*, 1978; *Thompson et al.*, 1979; *Reeves et al.*, 1979]. The precipitation pattern over a broader region than the GATE ship array has been estimated from the infrared imagery of the geo-

synchronous SMS 1 satellite by *Woodley et al.* [1980] (Figure 3). Over the ship array, the satellite estimates agree reasonably well with the radar measurements and therefore appear to be a useful extension of the GATE precipitation pattern. This pattern confirms that the ship array was, in fact, in the maximum precipitation belt of the ITCZ.

2. Types of Clouds Occurring in the ITCZ

The types of clouds that formed within the portion of the ITCZ sampled by the GATE ship array have been determined from whole-sky camera photography obtained aboard four U.S. ships [*Holle et al.*, 1979] and one Soviet ship [*Bibikova et al.*, 1977]. *Simpson* [1976], *Borovikov et al.* [1978], *Peskov* [1980], and *Lebedeva and Zavelskaya* [1980] have all commented on the frequent presence of several cloud layers, including cumulus clouds with bases near 500 m and layer clouds with mid-tropospheric bases near 4 km. From the U.S. photographs, *Holle et al.* [1979] determined that the frequency of low clouds (including deep cumulus and cumulonimbus as well as stratus and stratocumulus) and rainfall duration were maximum just south of 7°-8°N. Combined middle and high clouds extended north of this zone in a manner consistent with the classic Hadley cell circulation, with poleward flow of air at upper levels from the equatorial trough.

3. Contributions of Cloud Clusters to Cloudiness in the ITCZ

Trajectories of cloud clusters over West Africa and the tropical Atlantic during GATE were compiled by *Martin* [1975] and were found to occur in an east-northeast to west-southwest band extending from the African continent to the ship array and then westward across the Atlantic (for example, the cluster trajectories for the first 15 days of GATE in Figure 4).
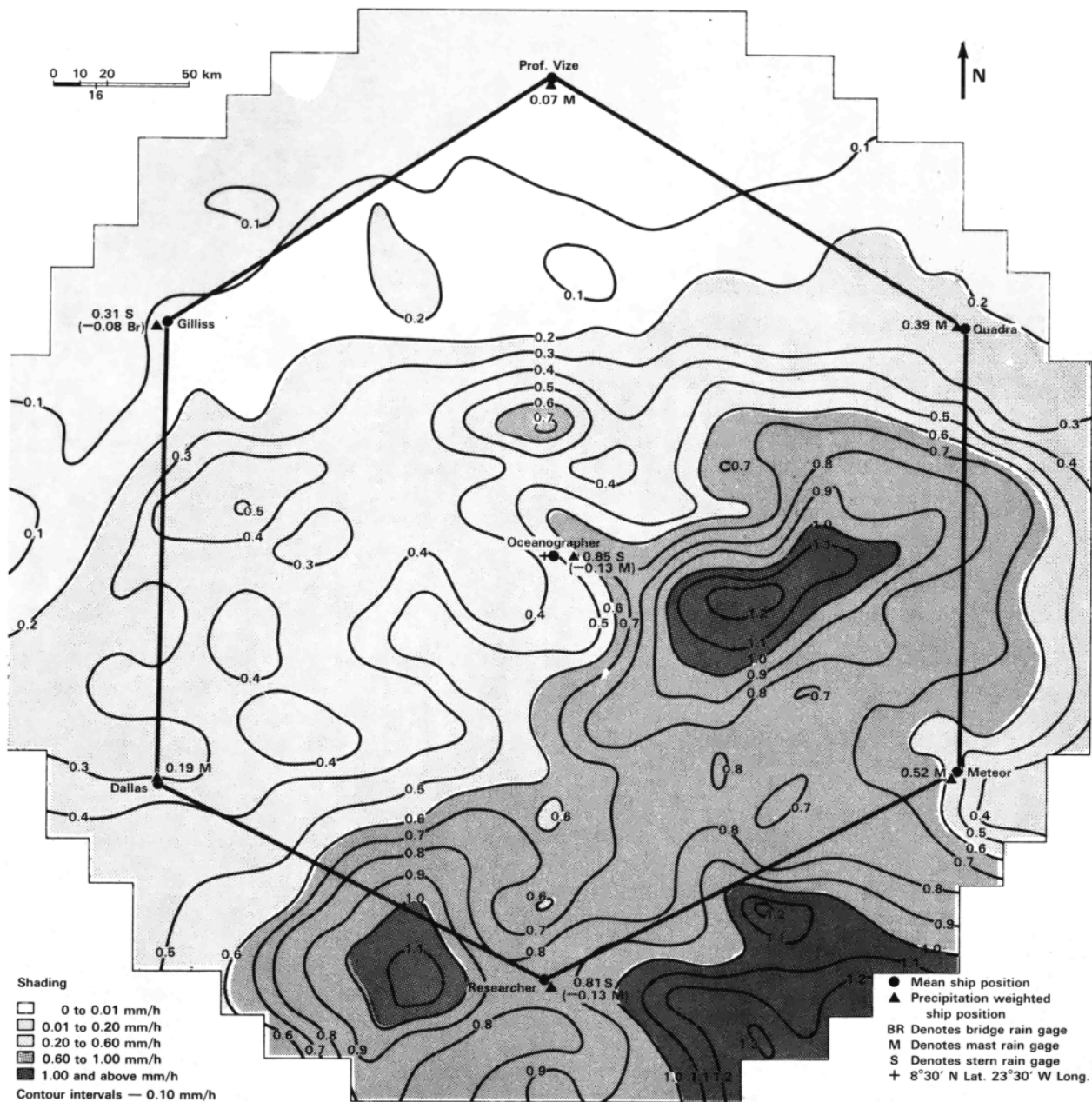
PHASE I ISOHYETAL MAP (June 28 - July 16)

Fig. 2.   GATE Phase I isohyetal chart derived from ship radar observations. The isopleths give the phase-mean rainfall
rates (mm h^{-1}). From Hudlow [1979].

Thus, Martin [1975] concluded, the GATE ship array 'lay squarely in the main cluster track and captured clusters in all stages of growth and dissipation.' The cluster tracks, moreover, coincided with the mean precipitation zone shown by radar and satellite (Figures 2 and 3), with the region of maximum cloudiness indicated by surface-based photography [Holle et al., 1979] and with global maps of cloud cluster frequency [Semyonov, 1975]. Clearly, the mean cloudiness and precipitation associated with the equatorial Hadley cell in the GATE region is largely a composite of individual cloud clusters.

A special type of cloud cluster is the 'squall line' or 'squall cluster' [Hamilton and Archbold, 1945; Zipser, 1969]. As noted by Martin [1975], squall clusters are evident in satellite imagery by their 'explosive growth, oval shape, and very high

brightness.' Aspliden et al. [1976] identified 176 squall clusters during GATE. The majority formed and decayed over the West African continent (162 and 130, respectively). Over the ocean, only 14 formed and 46 decayed. Thus the cloud clusters sampled by the GATE ship array were predominantly nonsquall clusters, while over the continent, cluster statistics, such as the higher cluster speed and longer trajectories seen over land in Figure 4, were strongly influenced by squall clusters.

4.   Modulation of Cloud Cluster Frequency by Synoptic-Scale Wave Passages

That cloud cluster frequency in the ITCZ can be modulated by the passages of easterly waves was shown by Reed and
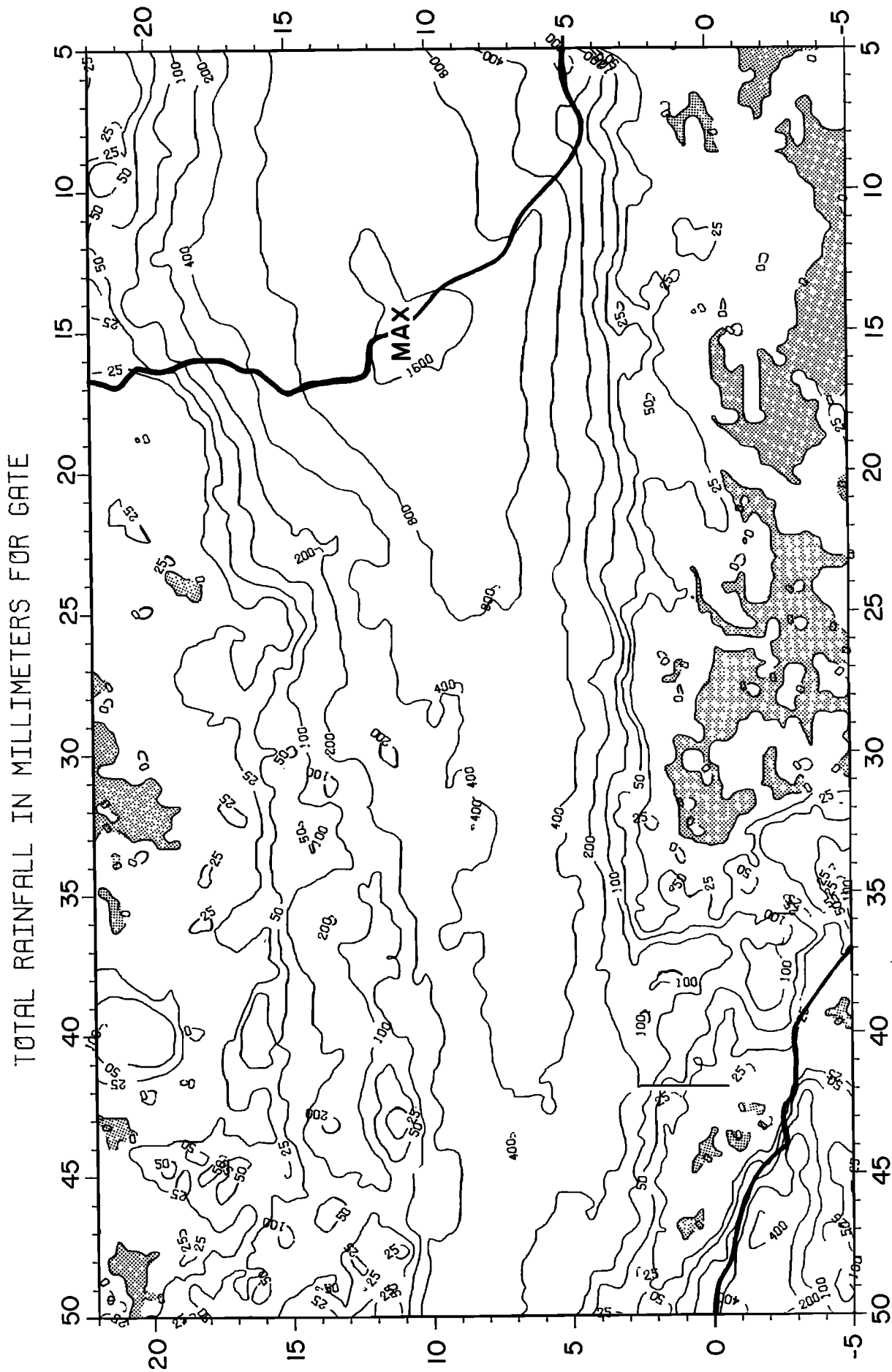
Fig. 3. Mapped total (mm) rainfall for all GATE (June 27 to September 20, 1974, excluding August 22). Tic marks indicate latitude (ordinate) and longitude (abscissa) in degrees. Coastlines indicated by heavy lines. Derived from SMS 1 satellite imagery. From *Woodley et al.* [1980].
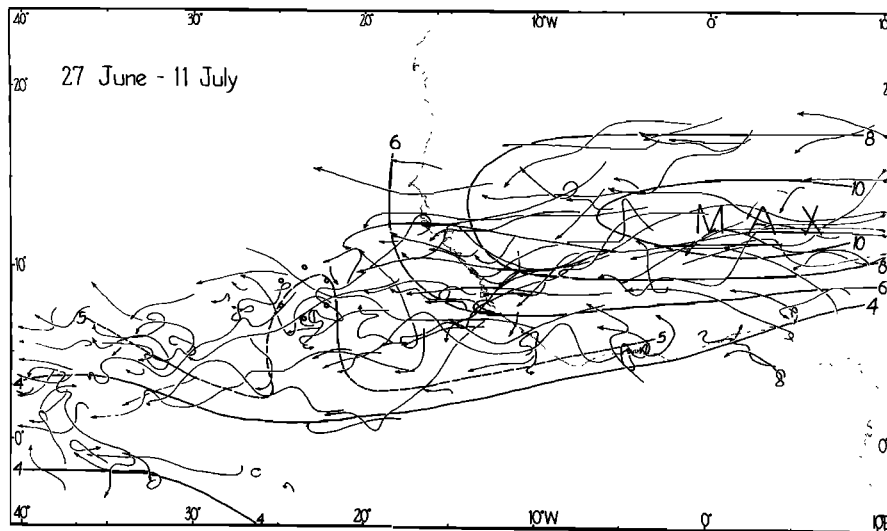
TOTAL RAINFALL IN MILLIMETERS FOR GATE

Fig. 4. Trajectories of cloud clusters for the first 15 days of GATE. Contours represent averages of cluster speeds over 10° × 10° squares. Circles indicate ship positions. (Reprinted with permission of *Martin* [1975].)

Recker [1971]. Synoptic-scale easterly waves were observed to pass over the GATE ship array at intervals of 3–4 days [*Burpee*, 1975; *Reed et al.*, 1977]. *Payne and McGarry* [1977] showed that the occurrence of convective cloudiness associated with clusters was enhanced at and ahead of trough axes and suppressed at and ahead of ridge axes (Figure 5). Large nonsquall cloud clusters occurred just ahead of the trough and moved at slightly less than the phase speed of the wave. Squall clusters also tended to occur just ahead of the trough

but moved at about twice the speed of the wave and tended to die just behind the ridge. The modulation of GATE cloud cluster occurrence by synoptic-scale waves is also indicated by the correlation of rainfall over the ship array with wave phase [*Thompson et al.*, 1979; *Hudlow*, 1979; *Reeves et al.*, 1979].

5. Diurnal Variation of Cloud Cluster Occurrence

Diurnal variations of convective cloudiness occur in the tropics for various reasons. Over continents, destabilization by

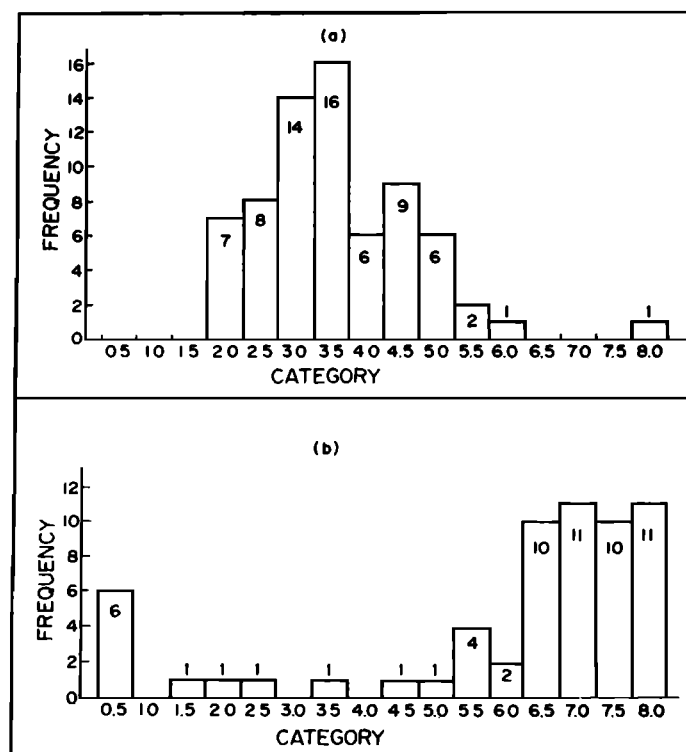Fig. 5. Frequency distribution of (a) maximum values of enhanced convective cloud coverage and (b) minimum values (representing supressed convective coverage) versus wave phase category for each separate positive andd negative region of coverage, respectively, during the 28-day period from August 23 to September 19, 1974. Category 4 is the trough, and category 8 is the ridge. From *Payne and McGarry* [1977].
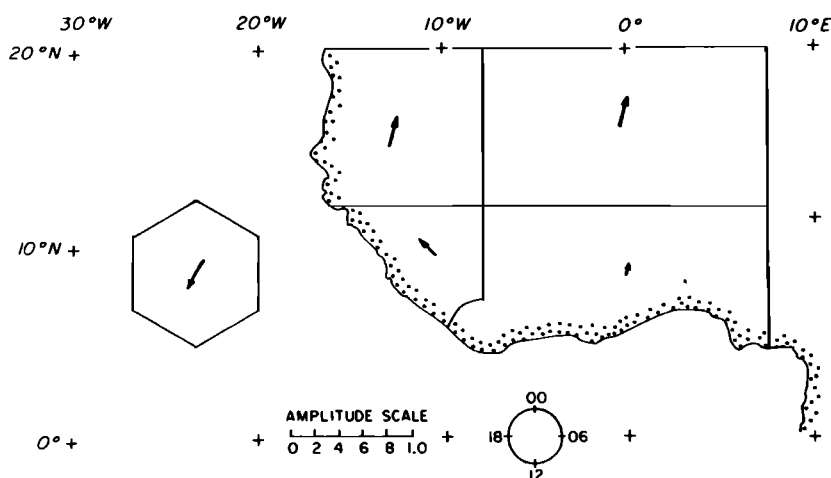
Fig. 6. Phase and normalized amplitude of diurnal cycle of convective cloudiness for Phases II and III of GATE based on 6-hour SMS 1 satellite photographs. Time of the maximum is indicated by direction of arrow according to 24-hour clock. From *McGarry and Reed* [1978].

the daily cycle of insolation can be important. Over and near large islands and peninsulas such as Borneo and Malaya, land-sea breezes control diurnal variations in clouds and precipitation [*Ramage*, 1971; *Houze et al.*, 1981]. Over much of the open equatorial oceans, there is a tendency for an early morning (≈0700 LST) maximum of precipitation, which *Gray and Jacobson* [1977] and *McBride and Gray* [1980] attribute to day-night differences in the radiative heating profiles in cloudy and cloud-free regions. They suggest that these differences lead, through adjustments of pressure fields, to a maximum of low-level convergence in the morning in the cloudy areas.

The diurnal variation of deep convective cloudiness inferred from satellite infrared images has been determined for the GATE ship area by *Gruber* [1976] and for both the ship area and portions of the West African continent by *McGarry and Reed* [1978], *Murakami* [1979], *Ball et al.* [1980], and *Griffith et al.* [1980]. *McGarry and Reed* [1978] also analyzed the diurnal cycles in rainfall data and reports of thunder and lightning. McGarry and Reed showed further how the amplitudes and phases of local diurnal cycles vary geographically over both the GATE ship area and the coastal and land areas of western Africa (see Figure 6). Afternoon maxima of convective cloudiness and precipitation occurred over the ship array, while over the northern part of the land area, large-amplitude cycles occurred, with rain amounts greatest shortly before midnight, maximum cloud cover shortly after midnight, and light rain most frequent near dawn.

The diurnal cycles over the northern continental regions are attributed by McGarry and Reed to the tendency noted by *Martin* [1975] and *Aspliden et al.* [1976] for intense cloud clusters to form in the afternoon and then take several hours to reach their stage of maximum development. The explanation of the afternoon maximum of cloudiness and precipitation over the GATE ship array is not as obvious. Noting *Cox and Griffith*'s [1979] finding of significant differences in day and night heating profiles in cloudy and cloud-free regions in the GATE area, *McBride and Gray* [1980] modify their explanation of the 0700 LST cloudiness maximum over other equatorial ocean areas by suggesting that the adjustment of pressure fields resulting from the radiative heating and cooling differences leads to enhanced convergence in the morning

but that the tendency for GATE cloud clusters (they say squall lines) to take several hours to reach their maximum stage of development explains the observed early afternoon precipitation maximum.

6. Sizes and Structures of Precipitation Areas in the ITCZ

In satellite imagery a cloud cluster typically appears as a rather homogeneous patch of upper level cloud. However, the precipitation falling from this cloud is seldom, if ever, correspondingly homogeneous. Typically, there are several cumulonimbus features with precipitation areas of a variety of sizes and types interconnected by the same upper cloud shield. Statistical studies of radar echo patterns have determined characteristics of the population of precipitation features that occurred in the GATE ship array.

a. The size spectrum of GATE radar echoes. Prior to GATE, convective radar echo patterns over the western tropical Atlantic Ocean had been studied by *Iwanchuk* [1973] and *López* [1976], who found that small echoes (<10² km² in area) dominated the total number of echoes, while large echoes (>10³ km² in area) accounted for most of the area covered by precipitation. Convection in GATE (i.e., the eastern Atlantic) has been found to be similar. Using radar observations from the GATE ship *Oceanographer*, *Houze and Cheng* [1977] made a comprehensive survey of radar echoes occurring around 1200 UT on most days of GATE. Some 67% of the echoes in GATE were <10² km² in area (D scale) and 25% were 10²-10³ km² (C scale), while only 8% were >10³ km² (B/C scale) (Figure 7). Yet 79% of the total area covered by echoes was covered by the B/C scale echoes (Figure 8). Hence the relatively few large precipitation areas present in GATE (and other tropical cloud populations) take on great importance when their areal extent is considered. *López* [1978], also working with the *Oceanographer* radar data from GATE, further showed that the largest 10% of the echoes accounted for 90% of the precipitation.

Examined in another way, the size spectrum of radar echoes in the tropics (whether measured in terms of echo areas, heights, durations, or rainfall intensities) is usually found to be basically log normal [*López*, 1976, 1977]. In GATE, log normality of the radar echo population has been found to hold both for long periods of time [*Houze and Cheng*, 1977;
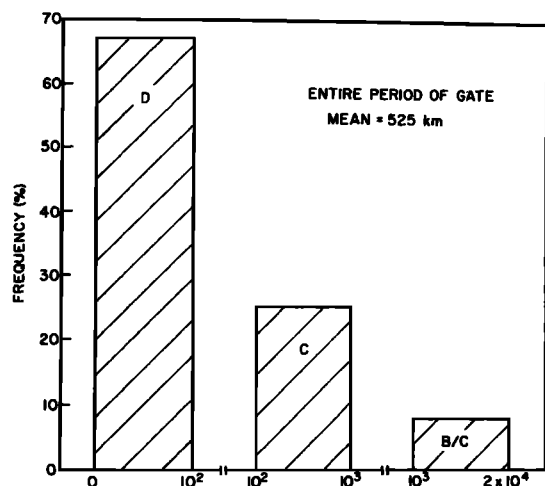
Fig. 7. Frequency of occurrence of D, C, and B/C scale radar echoes during GATE. From *Houze and Cheng* [1977].

López, 1978] (Figure 9) and at individual times during the development and dissipation of a single cloud cluster [*Warner and Austin*, 1978]. GATE shipboard observations indicate that visually observable cloud dimensions also had a log normal frequency distribution [*Kuusk et al.*, 1978].

Houze and Cheng [1977] found that echo heights and durations were positively correlated with echo areas and that larger echoes tended to contain multiple cores, with the most intense maxima occurring in the largest echoes (Figure 10). From Figure 10 it can be seen that on average only 10 or 11 echo cores were observed to exist at any one time in echoes exceeding 10^4 km^2 in area. If the individual cores were typically 10^2 km^2 in area, then only about 10% of the area covered

by these large echoes consisted of intense cores. Much of the area covered by these huge echoes consisted instead of relatively uniform rain in which individual echo cores could not be easily identified. It is evident from case studies of cloud clusters (section E) and observations such as those of *Borovikov et al.* [1975] that this uniform rain was of the type associated with the anvil cloud of the Line Islands cloud cluster studied by *Zipser* [1969].

b. Types of radar echoes in GATE. From the foregoing statistics of echo sizes, four types of GATE radar echoes (precipitation areas) can be identified: (1) isolated cells or cores—the smallest in horizontal extent (D scale to smaller C scale), shallowest in vertical extent (≤ 6 km), and least intense, (2) aggregates of cells or cores—of moderate horizontal extent (larger C scale and smaller B/C scale echoes), containing individual cores reaching 6–9 km in height, and having echo cores reaching moderate intensities, (3) aggregates of cells or cores with associated regions of uniform anvil rain—the largest echoes of GATE (larger B/C scale echoes), containing the deepest (generally >9 km, often overshooting to 16–17 km) and most intense cells, and (4) regions of uniform anvil rain containing few if any deep convective cells—remnants of type 3 echoes whose convective cells had died but whose anvil rain remained for some time.

These four types of echoes correspond to convection in successively more advanced stages of development. Type 3 and 4 echoes occurred only in major cloud clusters (see case studies in section E). Characteristics of the convective cells, which occurred in type 1, 2, and 3 echoes, will be discussed in section D6c, while the structure of the anvil precipitation will be described in section D6d.

c. Characteristics of cells. *López* [1978] examined a large sample of isolated cells and aggregates of cells (type 1 and 2 echoes). The frequency distributions of the maximum areas
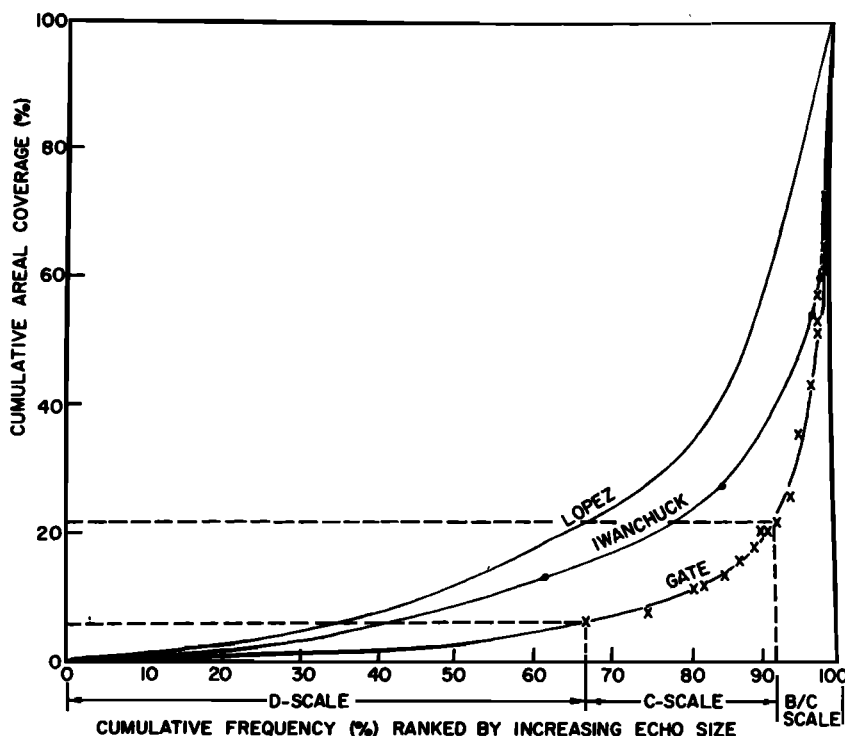

Fig. 8. Cumulative frequency distribution of accumulated echo areal coverage. Western tropical Atlantic distributions compiled by *López* [1976] and *Iwanchuk* [1973] are shown for comparison. From *Houze and Cheng* [1977].
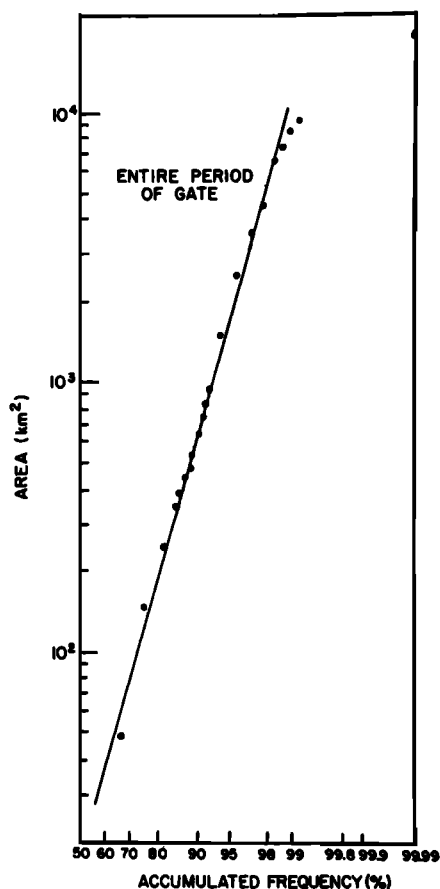
Fig. 9. Accumulated frequency distribution of areas covered by GATE radar echoes plotted in log-probability format. The straight line shows the log normal distribution computed from the mean (1.54) and standard deviation (0.83) of the logarithms of the observed echo areas. From *Houze and Cheng* [1977].
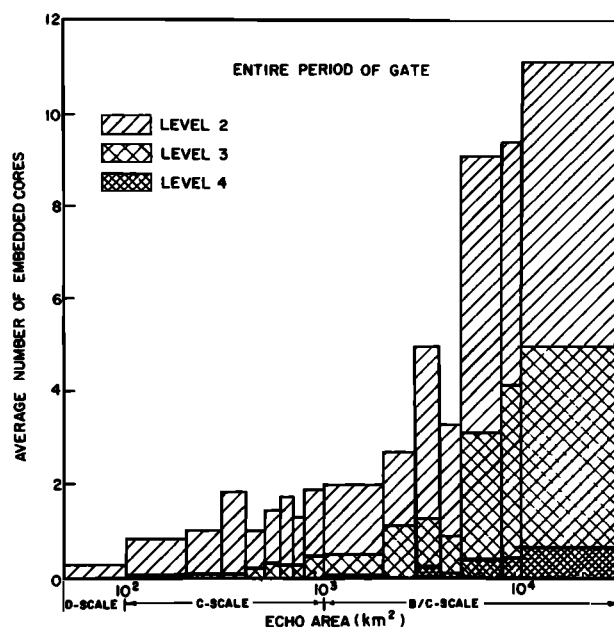

Fig. 10. Average number of embedded cores of maximum radar reflectivity located within GATE radar echoes in different size ranges. Shading indicates the fraction of the total number of cores in each size range which exceeded reflectivity threshold levels 2 (31 dBZ), 3 (30 dBZ), and 4 (47 dBZ). The unit dBZ, or decibels of Z, is a standard unit of radar reflectivity Z, given by dBZ = $10 \log_{10} Z$, where Z has units of mm^6/m^3. From *Houze and Cheng* [1977].

attained, durations and rainfall intensities of the isolated cells, and the cells contained in aggregates were determined. The distributions were found to be log normal for both the isolated cells and the cells making up aggregates (Figure 11). However, the means of the distributions for the cells in aggregates were greater, that is, the cells making up the aggregates tended to be larger, last longer, and rain more than isolated single-cell echoes. Evidently, as concluded by López, the formation of aggregates affords a measure of protection from entrainment of unsaturated environment air for cells embedded within the aggregates, while such protection is not available to isolated cells.

Direct sensing of the air motions in cells was accomplished by GATE aircraft sampling. *LeMone and Zipser* [1980] and *Zipser and LeMone* [1980] have examined aircraft measurements of the updraft and downdraft velocities in cells of type 1–3 echoes on 6 days of GATE. They divided the data into 'drafts,' where the vertical velocity is nonzero continuously for a flight path length ≥0.5 km, and 'cores,' for which the absolute values of the velocity exceed 1 m s⁻¹ for ≥0.5 km. The distributions of draft and core sizes and intensities were log normal at all altitudes in each echo system penetrated (Figure 12). The tendency of convective entities to be log normally distributed is thus seen to apply not only to gross echo structures from 10^2 to 5×10^4 km² in area (Figure 9), to echo cells ~10–200 km² (Figure 11), and to visible clouds [*Kuusk et al.*,

1978] but also to the individual updrafts and downdrafts ~0.25–50 km² in cross-sectional area that were embedded within the cells of the precipitating clouds.

The majority of the GATE convective cores described by *Zipser and LeMone* [1980] had mean vertical velocities of <3–5 m s⁻¹. (Peak values exceeded the mean values by a factor of 1.6 to 2.0.) In the middle troposphere, only 10% of the updraft cores had mean vertical velocities greater than 5 m s⁻¹ or diameters in excess of 2 km (Figure 12). Downdraft cores were weaker than updraft cores, except near cloud base, where updraft and downdraft cores were of similar intensity. In general, the GATE cores and drafts were similar in size and intensity to those observed in hurricanes but weaker than those observed in the continental thunderstorms observed in the U.S. Thunderstorm Project [*Byers and Braham*, 1949].
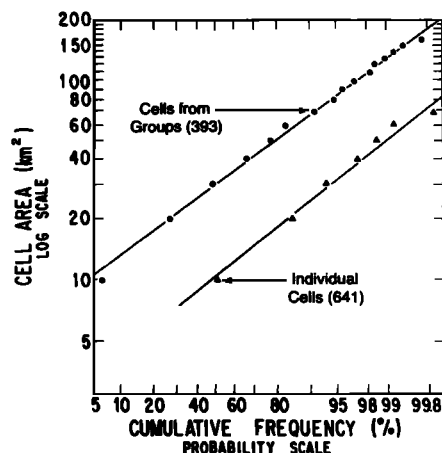

Fig. 11. Cumulative frequency distribution of the maximum area attained by radar echo cells that are isolated and members of aggregates. From *López* [1978].

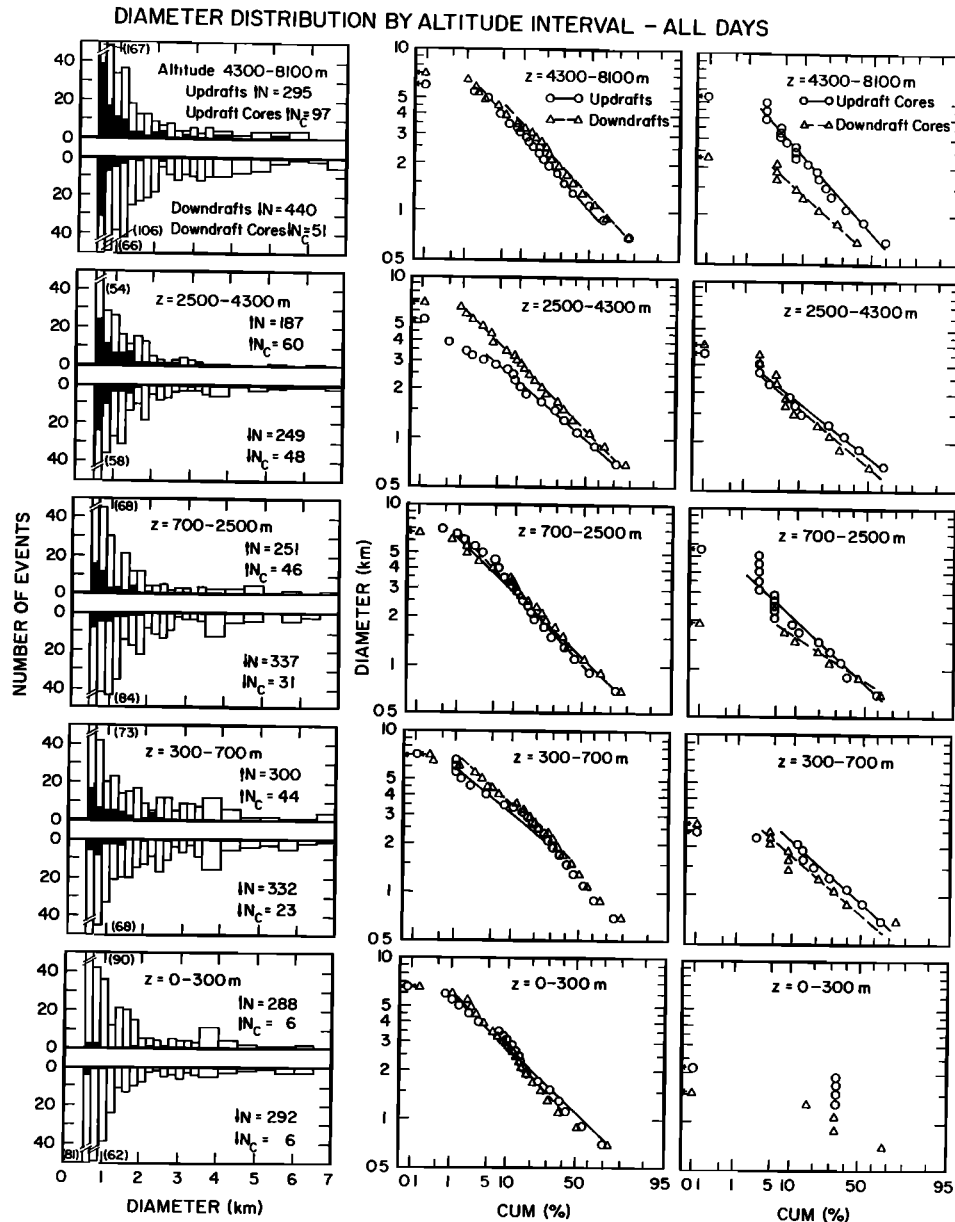DIAMETER DISTRIBUTION BY ALTITUDE INTERVAL - ALL DAYS

Fig. 12. Aircraft measurements in GATE convective cells. Combined draft and core statistics are summarized by altitude group. In bar graphs, total length is total number of drafts, and black is total number of cores. Cumulative distributions are in log-probability format. See text for definitions of drafts and cores. From *LeMone and Zipser* [1980].

d. Anvil precipitation structure. The anvil rain in type 3 and 4 echoes was a substantial contribution to the total GATE rainfall. *Cheng and Houze* [1979] estimated its contribution to be 40%. The structure of the anvil rain resembled that of mid-latitude stratiform rain. *Leary and Houze* [1979b] examined five examples of anvil rain. They found that the radar reflectivity was horizontally stratified with a well-defined radar bright band at the melting level (see Figure 13). Preliminary analyses of GATE radar measurements had indicated that bright bands were frequently present [*Houze*, 1975; *Shupiatsky et al.*, 1975, 1976a, b]. The presence of the bright band indicates that strong convective cells were absent and ice particles were gently settling downward, melting, and falling to the surface as widespread anvil rain.

The physical processes in an anvil rain region are illustrated schematically in Figure 14. The microphysical structure was deduced indirectly by *Leary and Houze* [1979b] from observed

vertical distributions of radar reflectivity and by determining the types of ice particles that would, upon melting, produce a population of raindrops having a size distribution similar to drop size distributions observed aboard GATE ships and aircraft [*Cunning and Sax*, 1977a, b; *Austin and Geotis*, 1979]. It was determined that rimed aggregates and hexagonal graupel were the probable ice particle types just above the melting layer. The existence of riming and graupel is consistent with the observations of *Borovikov et al.* [1978], who note aircraft icing and liquid drops coexisting with ice in GATE cirrus clouds. They noted, however, that at altitudes as high as 12-13 km, only ice was present. These observations suggest active anvil clouds, in which enough lifting is present to maintain liquid water in the presence of ice. Below the melting level, the primary microphysical process in the anvil region is evaporation of the falling raindrops in dry subsiding air below cloud base. Air motions within and below the anvil and their relation-
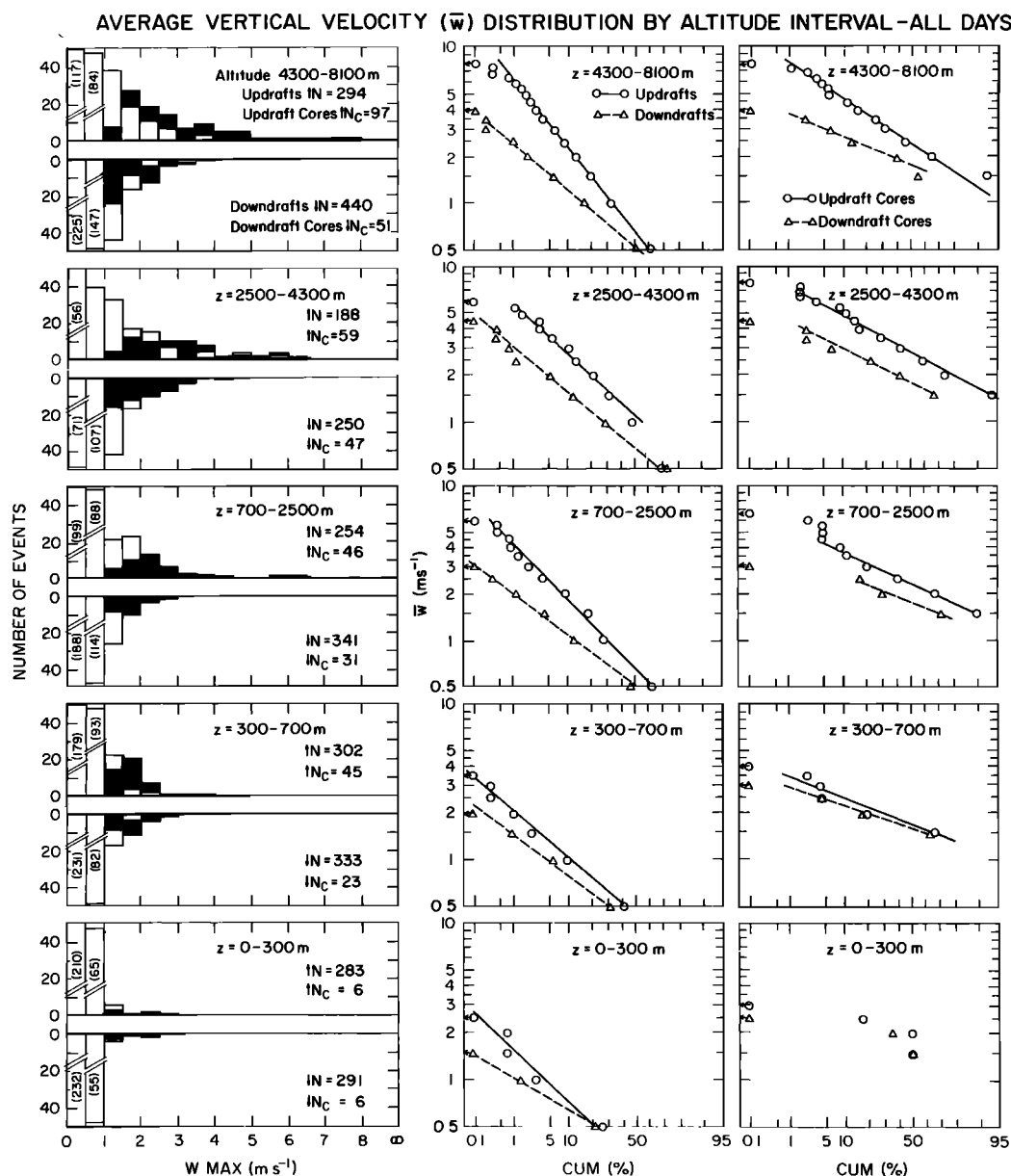
AVERAGE VERTICAL VELOCITY ($\bar{w}$) DISTRIBUTION BY ALTITUDE INTERVAL—ALL DAYS

Fig. 12. (continued)

E. CASE STUDIES OF GATE CONVECTION

In the preceding section it was seen that the mean cloudiness and precipitation in GATE were accounted for primarily by cloud clusters. To date, 12 GATE cloud clusters have been subjected to various degrees of case study analysis (Table 1). The first six case studies listed in Table 1 were of squall clusters. The other six were nonsquall clusters. In the following subsections we will first discuss the squall clusters. This will be followed by a discussion of the nonsquall clusters and then by a discussion of smaller cumulus and cumulonimbus associated with clusters.

1. Squall Clusters

a. The formation process. The statistical studies of *Martin* [1975] and *Aspliden et al.* [1976] showed that squall clusters

were most frequent over the African continent. In a case study, *Fortune* [1980] reported on a 'family' of five squall lines that developed in series over the African continent. The time lapse sequence of satellite imagery in this case shows the origin of each squall system and the westward advance of its anvil shield or its leading arc of low cumulus (Figure 15). In high-resolution visible imagery, available for the daylight hours, the arc clouds are seen at the squall front just ahead of the advancing upper level anvil cloud. The five squall systems were initiated from groups of or individual cumulonimbus identified in Figure 15 as A–C, D–F, G–H, K, and L. Each of these squall systems produced a distinct anvil whose rapid expansion was tracked and measured. Systems A–C and D–F developed almost simultaneously and eventually merged. The resulting combined squall system appeared to trigger or excite the development of the next system during its late stages, when it approached the developing cells G–H. In a similar way the squall that developed from G–H subsequently ap-
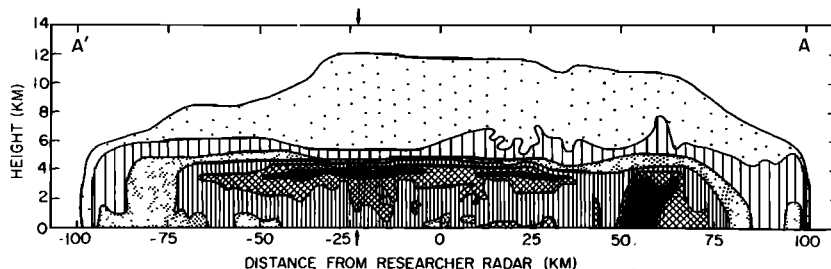
Fig. 13. Vertical cross section showing the uniform precipitation (between −150 and 50 km) in a large GATE radar echo. A radar bright band is in evidence in the melting layer just below 4-km height. Data were obtained with the *Researcher* radar at 2100 UT, September 4, 1974. The outside contour is for the minimum detectable echo, inner contours are for 23, 28, 33, 38, and 43 dBZ (dBZ is defined in the caption to Figure 10). From *Leary and Houze* [1979b].

peared to trigger two new squall lines, one to the south and one to the north, as it spread out and approached the cumulonimbus cells K and L.

The squall line system studied by *Houze* [1977] also formed at the advancing arc-shaped edge of a dissipating anvil cloud, in this case, one which had moved from northeast to southwest over the ocean from a position over Africa on the preceding day. Apparently, in addition to being favored ahead of the troughs of synoptic-scale waves or at certain times of the day (see sections D3–D5), new squall lines tend to become organized when cumulonimbus cells form along or just ahead of the edges of horizontally expanding pools of dense downdraft air deposited at the earth's surface by older cloud clusters.

b. *Squall line and anvil precipitation.* *Houze* [1977] used GATE radar data to document the evolution and internal structure of a cloud cluster, which conformed in general with *Zipser*'s [1969] conceptual model of a squall cluster and with the results of other pre-GATE studies of tropical squall lines [*Hamilton and Archbold*, 1945; *Eldridge*, 1957; *Tschirhart*, 1958; *Obasi*, 1974; *Betts et al.*, 1976]. The system consisted of a squall line forming its leading edge and a trailing anvil region. The radar data showed that the leading line consisted of dis-

crete line elements (LE's), which formed ahead of the squall line, weakened toward the rear of the line, and blended into the trailing anvil region as they dissipated. Each LE progressed through a period of rapid growth, with echo tops typically penetrating the tropopause to maximum heights of 16–17 km, then decreasing to heights of 13–14 km, corresponding to the height of the top of the anvil cloud with which the LE's merged at the end of their duration as active convective entities. This process is indicated schematically in Figure 16.

As the old squall line elements dissipated, their strong upward air motions apparently ceased and no longer carried precipitation particles upward or suspended them aloft. The fallout of particles from these weakened line elements then took on a stratiform appearance, and as the elements were incorporated into the anvil, they became indistinguishable from the rest of the anvil cloud and precipitation, which was horizontally stratified, with a pronounced melting band. This structure, illustrated schematically in Figure 16 and by actual example in Figure 17, is similar to that shown in Figures 13 and 14. The mature squall line system exemplifies the type 3 radar echoes that consisted partly of convective cells and partly of stratiform rain (section D6b). The anvil precipitation evolved

Fig. 14. Schematic vertical cross section and vertical profile of radar reflectivity (along dashed line A-A' in the cross section) in horizontally uniform precipitation associated with an anvil cloud. The anvil cloud occurs to the rear of intense convective cells propagating in the direction from right to left in the figure. The dark solid line is the contour of minimum detectable radar echo, lighter solid lines and shading indicate contours of higher reflectivity, and the scalloped line indicates the cloud boundary. From *Leary and Houze* [1979b].

TABLE 1. Studies of Major Convective Events in GATE

Investigator	Day of GATE	Type of Convective Event
Reed [1975] Zipser [1977]	June 28	squall line over the GATE ships
Houze [1975, 1976, 1977] Mansfield [1977] Leary and Houze [1979b, 1980] Ogura et al. [1979]	Sept. 4–5	squall line over the GATE ships
Zipser [1977] Fortune [1980]	Sept. 4–5	family of squall lines over Africa
Houze [1975] Mansfield [1977] Leary and Houze [1979b]	Sept. 11	squall line over the GATE ships
Houze [1975] Shupiatsky et al. [1976b] Mandics and Hall [1976] Zipser [1977] Mansfield [1977] Nitta [1977] Gaynor and Mandics [1978] Leary and Houze [1979b]	Sept. 12	squall line over the GATE ships
Houze [1975] Mansfield [1977] Leary and Houze [1979b]	Sept. 16	squall line over the GATE ships
Zipser and Gautier [1978]	July 15	nonsquall cloud cluster associated with an oceanic tropical depression northeast of GATE ships
LeMone [1975] Nicholls [1979]	Aug. 3	weak nonsquall cluster in an ITCZ wind pattern over the GATE ships
Shupiatsky et al. [1976b] Ogura et al. [1979]	Aug. 11–12	nonsquall cluster in a well-defined ITCZ cloud pattern over the GATE ships
Betts [1978] Mower et al. [1979] Warner [1980]	Sept. 2	nonsquall cloud cluster over the GATE ships
Leary and Houze [1976, 1979a, b] Suchman and Martin [1976] Nitta [1977] Ogura et al. [1979] Leary [1979] Nicholls [1979] Sikdar and Hentz [1980]	Sept. 5	double nonsquall cloud cluster over the GATE ships
Zipser [1980] Zipser et al. [1981]	Sept. 14	nonsquall cloud cluster over the GATE ships
Suchman et al. [1977] Warner and Austin [1978] Warner et al. [1979] Warner et al. [1980] Simpson and van Helvoirt [1980]	Sept. 18	nonsquall cloud cluster and associated small clouds over the GATE ships

as shown in Figure 18. During the first few hours of the disturbance, little anvil rain fell. As the anvil developed and expanded, the amount of rain falling from it became approximately equal to that coming from the squall line itself.

c. *Convective and mesoscale vertical motions.* The large portion of the total rain coming from the anvil indicates that mesoscale vertical air motions associated with the anvil cloud as well as convective-scale updrafts and downdrafts associated with the cumulonimbus elements making up the squall line itself were important dynamical components of the squall line

system. Essentially similar conceptual models of the convective-scale and mesoscale vertical motions in GATE squall line systems have been presented by Zipser [1977, Figure 19], Houze [1977, Figure 16], and Leary and Houze [1979b, Figure 14]. These models are consistent with the Venezuelan squall line model of Betts [1976a] and Betts et al. [1976]. The updraft and downdraft structures contained in the models are summarized in the following subsections.

d. *Convective-scale updrafts.* Convective-scale updrafts occur in the cumulonimbus elements making up the squall
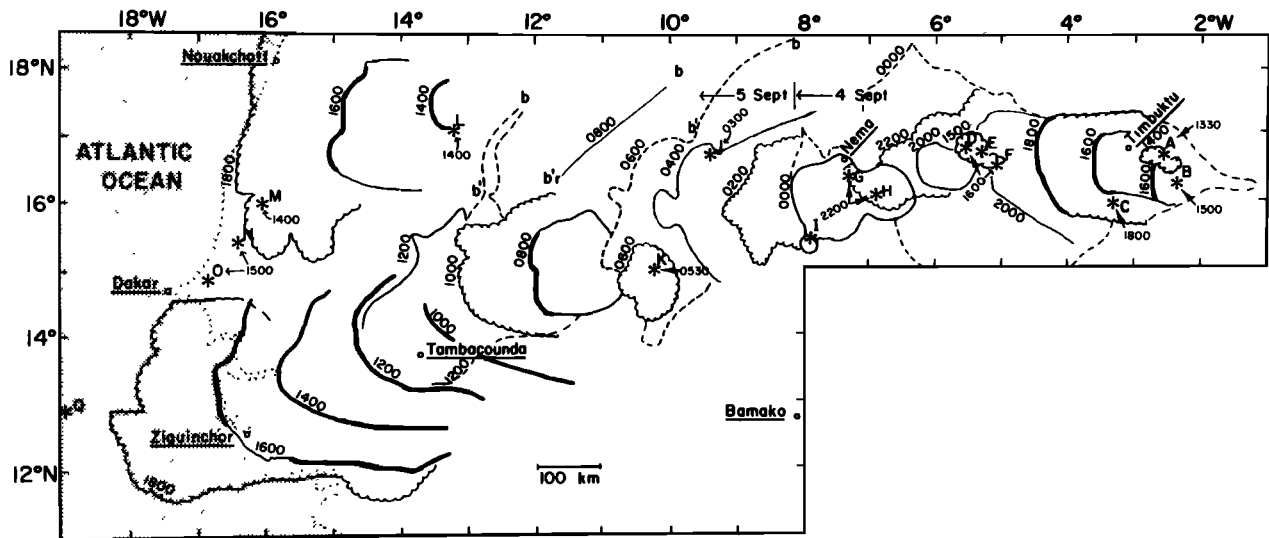
Fig. 15. The advance of the squall line family of September 4 and 5, 1974, from its origins to the Atlantic. Asterisks mark the points of origin of squall line elements A-Q, with the hour of origin indicated. Alternating scalloped and thin lines show the leading edge of the anvil cloud at 2-hour intervals. Thick solid curves mark the position of the arc front on the visible pictures. Dashed lines outline the anvil every 6 hours. Line b-b' is a long-lived but dormant arc of middle cloud. From *Fortune* [1980].

line. The rapid growth of the radar echoes traced through their life history to typical maximum heights of 16–17 km by *Houze* [1977] clearly indicates that buoyant convective updrafts produced these cells. The air feeding the squall line updrafts comes from the presquall boundary layer. The vertical structure of the squall line convective elements, shown by radar data [*Houze*, 1977] and in satellite imagery [*Fortune*, 1980], shows that these updrafts have a distinct tilt.

e. *Convective-scale downdrafts.* Just behind and below the sloping updraft of a squall line element there is a concentrated downpour of heavy precipitation that contains a convective-scale downdraft. These downdrafts, which are characteristic of cumulonimbus, apparently are negatively buoyant, nonhydrostatic features composed of air, whose downward motion is initiated by the weight of hydrometeors and sustained by evaporation.

The air feeding the convective-scale downdrafts comes from levels between 900 and 600 mbar. At these levels the mean relative flow is toward the squall line. Consequently, air enters one of these downdrafts after either circumnavigating discrete updraft towers distributed along the squall line or by finding itself behind a new line element that formed just

ahead of the current squall line as part of the line's discrete propagation.

When the convective downdraft air reaches the surface, it has a lower moist static energy and is more stable that the presquall boundary layer air [*Betts*, 1976a; *Gaynor and Ropelewski*, 1979; *Fitzjarrald*, 1979; *Barnes*, 1980]. This air spreads out, partly toward the front of the squall line system and partly toward the rear. The forward spreading portions of the downdraft outflows of the various cumulonimbus elements along the squall line typically intersect and form a continuous windshift line along the front of the squall system in the manner suggested by *Byers and Braham* [1949] for mid-latitude squall lines (see their Figure 113).

The portion of convective-scale downdraft outflow that spreads toward the rear of the squall line system streams out in a thin layer 50–500 m above the surface. As this layer of cold air moves out over the warm sea surface, enhanced activity of turbulent plumes rising from the surface occurs [*Mandics and Hall*, 1976; *Houze*, 1977; *Zipser*, 1977; *Gaynor and Mandics*, 1978; *Gaynor and Ropelewski*, 1979; *Fitzjarrald*, 1979]. The mixing associated with the plumes acts to raise the moist static energy of the convective downdraft air and thereby gradually

Fig. 16. Schematic cross section through squall line system. Streamlines show flow relative to squall line. Thin dashed streamlines show convective updraft circulation, thin solid streamlines show convective-scale downdraft circulation associated with mature squall line element, and wide arrows show mesoscale downdraft below the base of the anvil cloud. Wide, dashed arrows show mesoscale ascent in the anvil. Dark shading shows strong radar echo in the melting band and in the heavy precipitation zone of the mature squall line element. Light shading shows weaker radar echoes. Scalloped line indicates visible cloud boundaries. Adapted from *Houze* [1977].

Fig. 17. Vertical cross section through entire squall line system, along azimuths 223° (SW) and 43° (NE) from *Oceanographer* radar at 1545 UT, September 4, 1974. Inside contours are for 38, 33, 23 dBZ and minimum detectable echo (dBZ is defined in the caption to Figure 10). Outside scalloped contour outlines cloud boundary estimated from infrared satellite imagery. From *Houze* [1977].

convert it to air with properties characteristic of the undisturbed (or presquall) subcloud layer. This recovery is sufficiently slow that the surface outflow layer, or squall line 'wake,' is evident for up to sev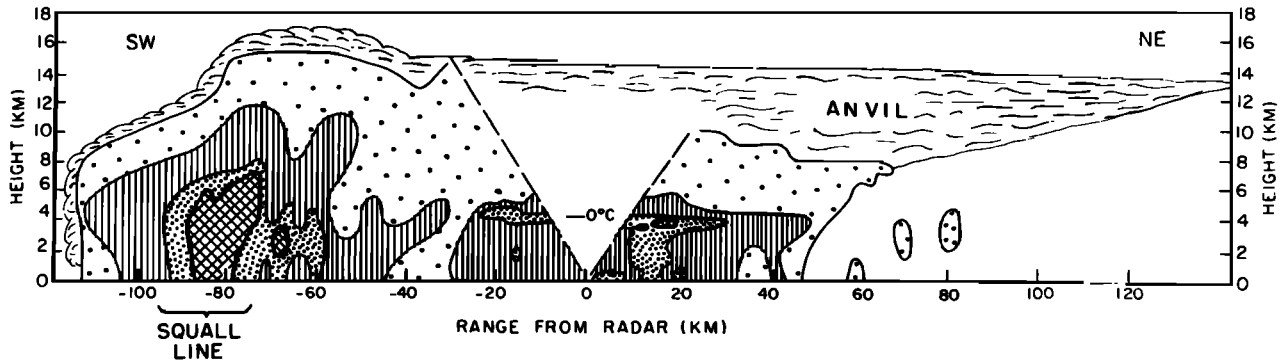eral hundred kilometers behind the squall line (Figures 16 and 19). This surface outflow layer (see next section) is bounded above by a stable layer maintained by widespread subsidence below the anvil cloud. The subsiding air is characterized by low moist static energy, and its entrainment across the stable layer helps slow the recovery of the surface wake to presquall conditions.

f. The mesoscale downdraft. The subsiding air below the anvil extends over horizontal scales of 100–500 km. By mapping the surface outflow pattern of the September 12 GATE squall line system, *Zipser* [1977] estimated the downward velocity at 500 m, near the top of the wake layer, to be 5–25 cm s⁻¹ (Figure 20). A downdraft of this horizontal scale and magnitude is a hydrostatic circulation feature, in contrast to the nonhydrostatic convective-scale downdrafts associated with the cumulonimbus rain showers making up the squall line. *Zipser* [1969] proposed that the wide hydrostatic (or mesoscale) downdraft below the anvil of a tropical squall line was thermally driven by the evaporation of rain falling from the mid-tropospheric base of the anvil. Using a hydrostatic mesoscale numerical model in which both cumulus-scale convection and cloud microphysical processes were parameter-

ized, *Brown* [1979] demonstrated that this mechanism was feasible for a tropical squall system. His model produced an anvil below which evaporative cooling led to adjustment of the mid-to-low tropospheric pressure field. The associated ageostrophic wind was convergent near the base of the anvil and divergent at the sea surface, and the mesoscale downdraft was located in the intervening layer. The melting of ice particles that produces radar bright bands near the bases of anvils was not included in Brown's model, but in real cases this melting reinforces the evaporative cooling in maintaining the mesoscale downdraft [*Leary and Houze*, 1979b].

The thermodynamic structure of the mesoscale downdraft has been documented by *Zipser* [1969, 1977]. He compiled the seven soundings shown in Figure 21, which were obtained beneath various tropical squall line anvils. Below the base of the anvil (about the 650-mbar level) the soundings show the warming and drying effects of subsidence with a maximum separation between temperature and dew point being reached near 900 mbar, at the top of the stable layer bounding the top of the surface wake. The warm dry air just above the wake has about the same value of moist static energy as the air near the base of the anvil. Building on ideas of *Betts and Silva Dias* [1979], *Leary* [1980] used a one-dimensional steady state, hydrostatic model of a downdraft containing a realistic spectrum of evaporating raindrops to show that the soundings below

Fig. 18. Total rain integrated over areas covered by squall line and anvil portions of a squall line system. Circled points refer to squall line region. Data points derived from *Oceanographer* radar echo patterns are indicated by pluses. Points derived from composite *Oceanographer* and *Researcher* radar echo patterns are indicated by dots. Points derived from composite *Oceanographer*, *Researcher*, and *Gilliss* echo patterns are indicated by crosses. From *Houze* [1977].

TOPS ≈ 200 mb OR HIGHER

AMBIENT
UPPER TROP
AIR
(21)

NEW
TOWERS
(22.5)

OLD
TOWERS
(22.5)

ANVIL
6-10 km
THICK

OLDER
TOWERS

STRONGEST
UPDRAFTS

(21.5)

MESOSCALE ASCENT

MELTING SNOW —0°C—

AMBIENT LOW θ_w AIR
(19)

DILUTED UPDRAFTS
(22.5)

AMBIENT
LOW θ_w
AIR
(19)

"CROSSOVER
ZONE"

MESOSCALE
UNSATURATED
DOWNDRAFTS

STABLE LAYER TOP (1000-1500 m)

AMBIENT CLOUD LAYER AIR
(21)

SATURATED
CONVECTIVE
SCALE
DOWN-
DRAFTS
(21.5)

MESOSCALE
DESCENT
(19.5)

WARM, DRY

AMBIENT SUBCLOUD AIR
(23.5)

COOL,
SATURATED
(21.5)

STABLE LAYER BASE (100-400 m)

(20.5)

Minimum Dew Point

MESOHIGH

MESOLOW

SQUALL FRONT

50 km　　　100 km

Fig. 19. Schematic cross section through a class of squall systems. All flow is relative to the squall line, which is moving from right to left. Circled numbers are typical values of wet-bulb potential temperature in degrees Celsius. From *Zipser* [1977].
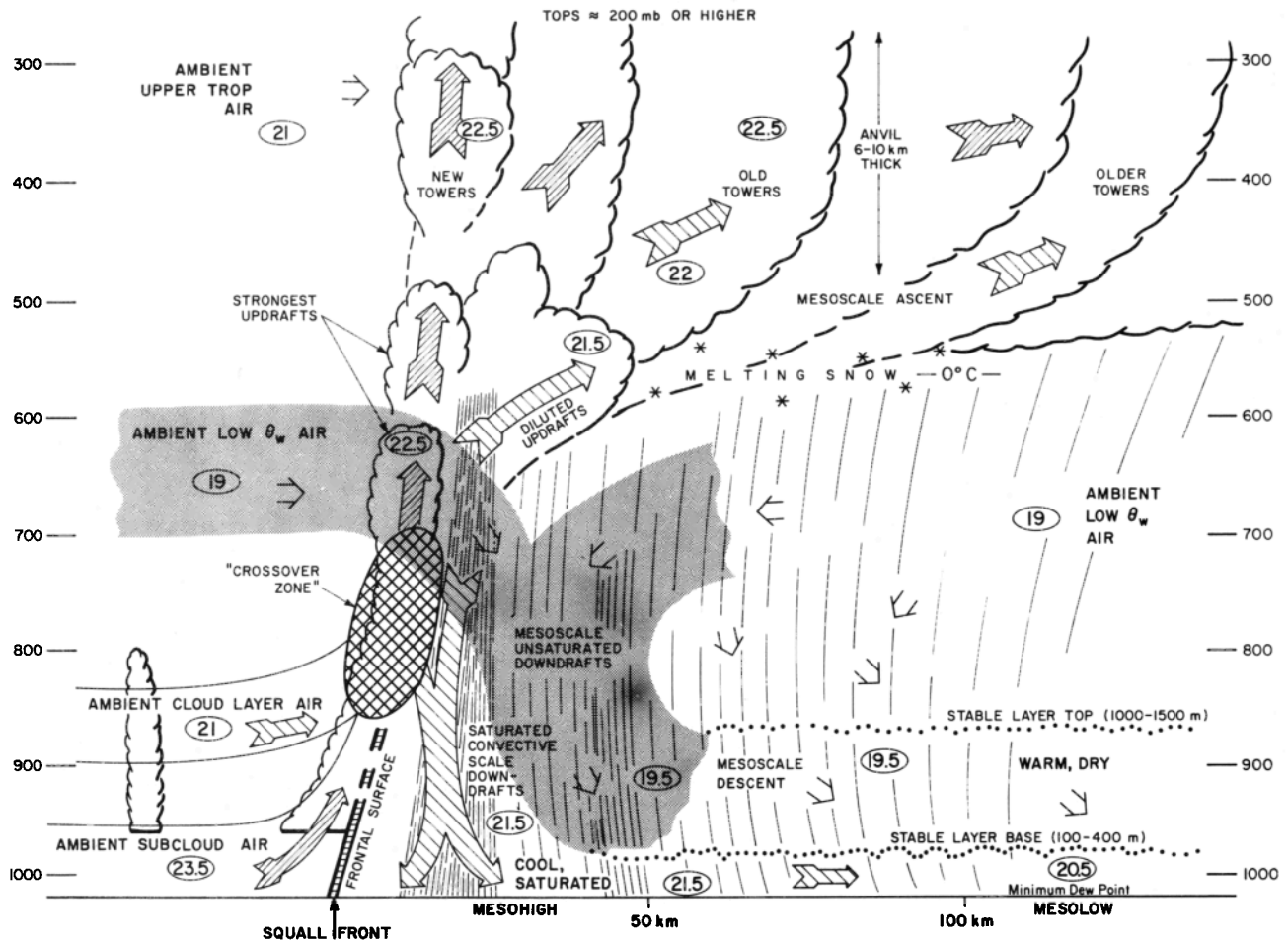
anvils result from an imbalance between the evaporation of the falling precipitation particles, which acts to increase the relative humidity, and the subsidence, which warms and dries the air.

While the cooling effects of evaporation and melting appear to support and maintain the mesoscale downdraft through hydrostatic adjustment of the pressure field below the anvil, the mechanism that initiates the mesoscale downdraft is not clear. *Miller and Betts* [1977] suggest on the basis of convective cloud model simulations that the mesoscale downdraft is forced to descend, since it overlies a spreading density current of convective-scale downdraft air. In a two-dimensional hydrostatic hurricane model with mesoscale (20 km) horizontal grid spacing, *Rosenthal* [1980] has shown that as high moist static energy air rising from low levels moves upward in the updrafts of squall-type features that form in the prehurricane stage, low moist static energy air carried downward in neighboring regions of compensating subsidence is advected into the lower part of the moist updraft. This air forms an unsaturated stable ascending wake which cuts the rising cloud air off from lower levels. The stable ascent in the wake leads to cooling below the cloud and a hydrostatic pressure rise at the surface. A mesoscale downdraft then forms at low levels and builds upward.

g. *The mesoscale updraft.* Within the anvil cloud itself, directly above the mesoscale downdraft, there appears to be a mesoscale updraft. Mesoscale ascent occurs in the anvil cloud in *Brown*'s [1979] numerical model and also in the anvil formed by the successive cutting off of rising cloud elements by the mesoscale updraft wakes in *Rosenthal*'s [1980] model. Similar mesoscale updrafts have been produced in mesoscale models simulating mid-latitude convective systems [*Kreitzberg and Perkey*, 1977; *Fritsch and Chappell*, 1980]. The mesoscale ascent in these models is hydrostatic and driven thermally by condensation heating. Observational evidence consistent with (but not proving the existence of) such mesoscale updrafts in GATE squall line anvils includes (1) the large amount of rain falling from anvils [*Houze*, 1977], (2) divergent and anticyclonic 200-mbar-level outflow centered in anvil cloud regions [*Houze*, 1977; *Fortune*, 1980], (3) indications that liquid water existed in anvils [*Borovikov et al.*, 1978; *Leary and Houze*, 1979b], (4) average upward motion on the resolvable scale of rawinsonde data centered on the anvil clouds of squall line clusters [*Frank*, 1978; *Betts*, 1978; *Ogura et al.*, 1979], and (5) mid-latitude squall line systems that exhibit mesoscale ascent in their anvils [*Sanders and Paine*, 1975; *Sanders and Emanuel*, 1977; *Ogura and Chen*, 1977; *Ogura and Liou*, 1980]. Work in progress at several institutions indicates that compositing of upper wind observations obtained in the vicinities of squall line anvils will prove the existence of the mesoscale updraft.

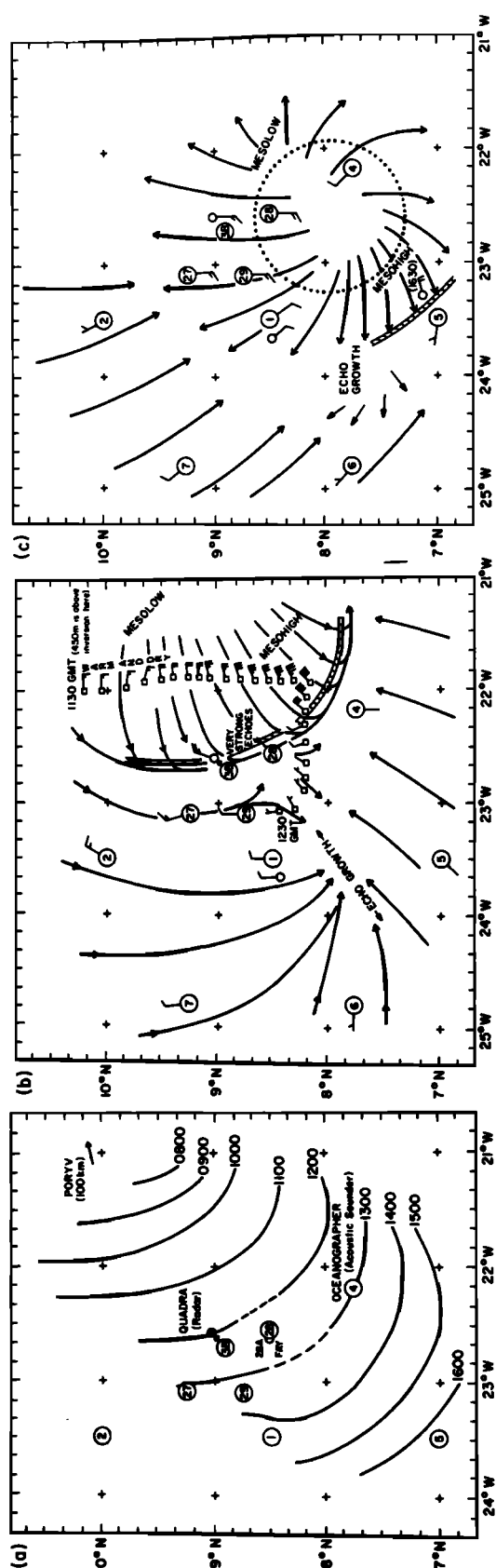h. *The mesoscale wind field near squall clusters.* The

Fig. 20. Aspects of the September 12, 1974, squall line in the GATE ship network. (a) Isochrone chart of the leading edge; dotted lines are used to indicate ambiguous squall line location due to interaction with preexisting line of convection. (b) Surface chart, 1200 UT, with some winds from the NCAR Electra at 450 m included. (c) Surface chart, 1600 UT, showing 150-km circle over which divergence is estimated at 2 × 10⁻⁴ s⁻¹. Each full wind barb is 5 m s⁻¹. From Zipser [1977].

squall cluster's circulation pattern (Figures 14, 16, and 19) can have a substantial imprint on the horizontal wind field over an area ~1000 km in dimension centered on the cluster. *Tourre* [1979] identifies a 'squall line wave' (wavelength about 1200 km) in the vicinity of squall clusters. In other studies, wind patterns are noted in relation to the anvil cloud. At the surface, directly below the anvil, anticyclonic divergent outflow predominates (Figure 20). Near the base of the mature anvil (600–700 mbar) a convergent circulation develops; for example, the September 4 oceanic squall [*Houze*, 1977] and the September 5 African squall [*Fortune*, 1980] exhibited convergent cyclonic rotation in the 700-mbar flow at the base of mature anvils. At upper levels (~200 mbar), divergent outflow was centered on the anvils [*Houze*, 1977; *Fortune*, 1980]. The pattern of divergence at low levels, convergence in mid-levels, and divergence at high levels in the anvil region is apparently associated with the mesoscale downdraft below the base of the anvil and mesoscale ascent in the anvil cloud itself.

i. Squall line propagation. Why squall clusters take on a mesoscale organization in which their convective cells line up and move as a group faster than other forms of convection in GATE and indeed often faster than the presquall environmental wind at any altitude is a question to which there is not yet a definitive answer. However, several recent theoretical studies provide insight and appear to be consistent with GATE and other tropical observations. Before summarizing these studies we note that the squall propagation cannot be explained by the density currents formed by the downdrafts of the convective cells within the squall line. These downdrafts are on the scale of the individual cells, while the mechanism that organizes the group of cells into a larger propagating line is necessarily mesoscale. Nor can the line's organization be explained by the mesoscale downdraft that spreads out below the squall's trailing anvil cloud, at least not in the initial stages of the line, since the arc-shaped squall line takes shape well before the development of significant anvil structure [*Houze*, 1977; *Fortune*, 1980].

Extending the work of *Raymond* [1975, 1976], *Silva Dias* [1979] used a model to show that a small initial convective perturbation in a mean GATE wind environment leads to the development of a propagating gravity wave structure on the scale of a tropical squall line. The wave develops arc-shaped horizontal structure (even though the basic state wind has no horizontal shear) and exhibits vertical tilt consistent with tilts observed in GATE squall lines [*Houze*, 1977; *Fortune*, 1980]. The wave is also consistent with the tendency, noted by *Houze* [1977], of tropical squall lines to move in part by discrete propagation. If the speed of the wave giving rise to the line organization exceeds the speed of individual cells, whose motion is probably controlled by their internal dynamics (for example, by the density current action of the convective-scale downdrafts), new cells would be expected to be triggered ahead of old ones as the wave continually moves ahead of existing cells.

Moncrieff and Miller [1976] inferred a squall line propagation speed by seeking the set of streamlines through a squall line that optimizes the upward flux of buoyancy and consequent release of kinetic energy by the system (for further discussion, see *Lilly* [1979]). The propagation speed associated with the optimal streamlines is related to the total potential energy available for release from an upstream parcel lifted from the surface. *Betts et al.* [1976] found that Venezuelan squall lines tended to travel with such a speed and that ob-
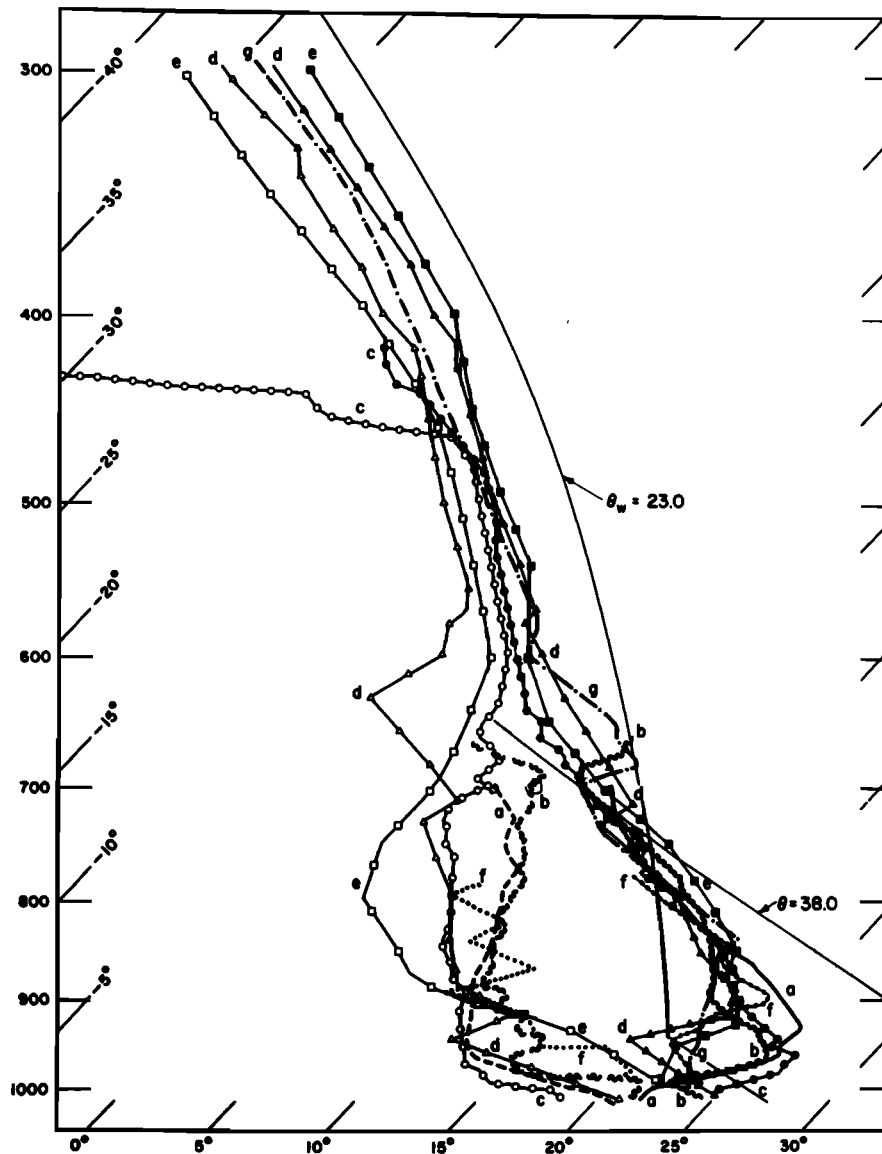
Fig. 21. Characteristic soundings of temperature and dew point in postsquall regions: (a) mostly in rain; (b) behind leading edge and 50 km behind trailing precipitation; (c) behind trailing precipitation; (d) behind leading edge and 174 km behind trailing precipitation; (e) 50 km behind trailing precipitation; (f) postsquall; (g) postsquall (no dew point available). From Zipser [1977].

served vertical profiles of horizontal wind differences (upstream minus downstream values of a given altitude) were consistent with the theoretically optimal streamlines. GATE squall lines exhibited upstream-downstream wind differences similar to the Venezuelan squalls [Houze, 1977; Fortune, 1980].

Another idea relevant to discrete propagation is mesocyclogenesis resulting from compensating downward motion [Fritsch, 1975; Hoxit et al., 1976; Fritsch and Chappell, 1980]. This process occurs in Rosenthal's [1980] two-dimensional hurricane model wherein the prehurricane squall line propagates in steps. The warming of the air column ahead of an active squall line element by compensating downward motion leads to lowering of the surface pressure ahead of the line. The convergence into this low is associated with a reversal of the low-level vertical motion, and a new squall line element forms there. It is interesting that compensatory downward

motion also is concentrated just ahead of the Silva Dias [1979] gravity wave squall line.

2. Nonsquall Clusters

As noted in section D3, the overwhelming majority of cloud clusters over the GATE ship array consisted of nonsquall clusters, which traveled more slowly than squall clusters and did not possess the distinctive oval cirrus shield or arc-shaped leading edge characteristic of squall systems. Despite these differences in motion and appearance the nonsquall and squall clusters in GATE exhibited surprising similarities in other aspects of their structures. In view of these similarities, much of the understanding of squall clusters reviewed above is basic to a universal understanding of convection in the ITCZ. The summary of GATE studies of nonsquall clusters presented below is organized around the theme of their struc-

tural and dynamical similarities to squall clusters. Their differences from squall clusters will also be discussed.

a. *Occurrence of mesoscale precipitation features in nonsquall clusters.* The GATE nonsquall clusters examined in case studies (Table 1) all contained mesoscale rain areas. *Leary and Houze* [1979a] extended the conceptual model of a tropical squall line system (Figures 14, 16 and 19) to describe the structure and behavior of these rain areas. They arrived at the more general concept of a mesoscale precipitation feature (MPF), of which the rain area of a squall cluster is an example but which also applies to the rain areas of nonsquall clusters.

b. *Typical life cycle of a mesoscale precipitation feature.* Squall clusters and some nonsquall clusters contain just one MPF. Other clusters contain several MPF's interconnected by a common anvil cloud. Intersections and mergers of the MPF's can add complexity to the precipitation pattern of the cluster. However, when the individual MPF's making up the pattern are identified and followed in time, they each exhibit a life cycle similar to that of a squall line MPF. This characteristic cycle, as postulated by *Leary and Houze* [1979a], is illustrated schematically in Figure 22.

In its formative stage (Figure 22a) the MPF appears on radar as a group of isolated type 1 (D scale or small C scale) radar echoes, which may be randomly distributed in the horizontal or arranged in a line. Figure 22 follows the evolution of a line. In squall clusters, and in many nonsquall clusters, such as those of July 15 and September 2, 5, and 14 (see papers referred to in Table 1), the MPF's are linear. The September 18 GATE cloud cluster, however, contained mesoscale features composed of groups of cells which tended to be randomly distributed [*Warner et al.*, 1980].

In the intensifying stage of an MPF the rain areas of the individual cells grow and merge (Figure 22b). The feature then comprises a single type 2 (large C scale or small B/C scale) radar echo.

The mature stage of an MPF is reached when a stratiform precipitation area develops from older cells blending together as they begin to dissipate (Figure 22c). In the same way that squall line elements weaken, become stratiform, and are incorporated into their associated anvil region (section E1b), convective cells of the MPF go through life cycles at the end of which they weaken and become components of a mass of stratiform precipitation falling from the middle-level base of the general anvil cloud of the cluster. For example, the cell at 9°N in Figure 23 was weakening. By 1215 UT a melting layer was evident near a height of 4 km, and the cell had taken on the character of light anvil rain. When several neighboring cells reach this stage, they become indistinguishable from each other and together can form an extensive region of stratiform anvil rain with a continuous melting layer. Though in weaker clusters the size of the stratiform regions that develop in this way may be limited (as on September 18; see *Warner et al.* [1980]), stratiform areas as great as 200 km in horizontal dimension can occur (Figure 13).

As long as new convective cells continue to form adjacent to a stratiform region, the mesoscale precipitation feature remains an aggregate of cells with an associated region of stratiform rain and as such composes a type 3 radar echo. A common way that a mature mesoscale precipitation feature continues forming new cells is by discrete propagation in a direction opposed to the relative wind at low levels. *Byers and Braham* [1949, pp. 78–79] found that in mid-latitude thunderstorms the probability of new cell development is (1) greatest

within the zone of overlap of downdraft outflows from neighboring convective cells and (2) greater in the leading and lateral sectors of cell groups than in the trailing portions of the groups. Applying similar ideas to a line of echoes that evolves into a mesoscale precipitation feature of the type observed in GATE on September 5, *Leary and Houze* [1979a] noted that convergence and new cell formation are favored between and upwind of the existing cells. Using a three-dimensional cumulus model, with GATE wind and thermodynamic soundings from the moderately unstable day of September 18, *Simpson and van Helvoirt* [1980] showed that an individual deep cumulonimbus cell of the type in the cluster observed on that day indeed develops a downdraft outflow at low levels that 'acts as an obstacle with stagnation and strong convergence (10^{-3} s^{-1}) at its upwind edge.' This convergence would favor the growth of new towers at the edge of the cloud, leading to some propagation upwind. Moreover, 'the pressure field and the more favorable vertical stratification could cause new separate cumuli to spring up at horizontal distances of 10 km or more upwind from the old cloud.'

In the dissipating stage of the MPF (Figure 22d) the formation of new convective cells diminishes, and as described in section D6b, the feature tends to become a type 4 echo. The feature can persist in this form, i.e., as a large region of mostly stratiform anvil cloud and precipitation, for several hours after the demise of the convective cells [*Borovikov et al.*, 1978; *Leary and Houze*, 1979a]. Mesoscale ascent in the anvil cloud (Figure 14) probably helps to prolong the dissipating mesoscale precipitation feature.

c. *Similarity of air motions associated with squall and nonsquall mesoscale precipitation features.* The mesoscale precipitation features in the nonsquall clusters of July 15, September 2, September 5, and September 14 all exhibited air motions that resembled those of squall line systems. Convective-scale drafts were associated with the cells, while mesoscale drafts were associated with their stratiform rain areas.

On July 15, intense convective cells extended northward from the center of a tropical depression along a line of strong confluence and convergence of the low-level wind (Figure 24). Extending some 100 km west of the convective line was a region of lighter stratiform rain falling from an anvil cloud based in the middle troposphere and extending up to the tropopause. Aircraft penetration of the intense cells at the northern end of the convective line revealed a series of closely spaced, exceptionally intense convective-scale updrafts, each ~1–5 km wide with peak speeds of 10–15 m s^{-1}. Convective-scale downdrafts ($\leq$4 m s^{-1}) were also encountered in this group of cells. In contrast to these intense convective drafts the region of uniform anvil rain to the west was characterized at low levels by widespread divergence indicating the presence of mesoscale subsidence below the anvil cloud.

In the stratiform rain area of one of the mature mesoscale precipitation features observed in the September 5 nonsquall cloud cluster, aircraft observations, described by *Leary and Houze* [1979a], showed cool, dry air of low moist static energy at low levels, consistent with the presence of a mesoscale unsaturated downdraft maintained by melting and evaporation of the falling rain (as in Figure 14). In the convective cells at the leading edge of the same mesoscale precipitation feature, a low-level aircraft penetration confirmed the presence of a convective-scale downdraft outflow.

The September 2 and 14 features were propagating similarly to the idealized case in Figure 22. Aircraft penetrations
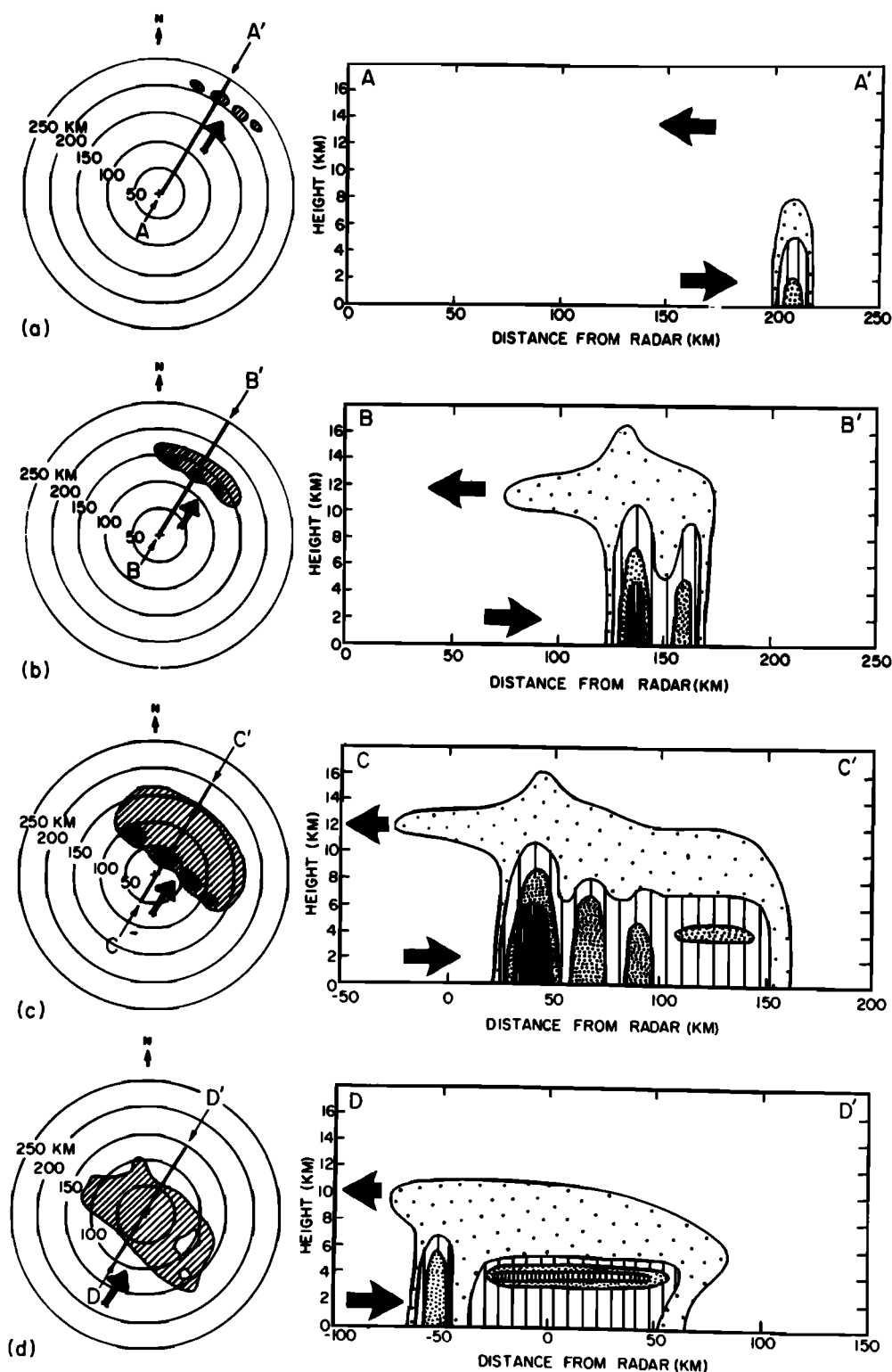
Fig. 22. Schematic of the structure of a mesoscale precipitation feature as viewed by radar in horizontal and vertical cross sections during the (a) formative, (b) intensifying, (c) mature, and (d) dissipating stages of its life cycle. The outside contour of radar reflectivity is the weakest detectable echo, and the inner contours are for successively higher reflectivity values. Heavy arrows on horizontal cross sections indicate direction of the low-level winds. Arrows on vertical cross sections indicate directions of the low-level and upper level winds relative to the feature. From *Leary and Houze* [1979a].

revealed convective-scale drafts of up to a few meters per second and gust fronts associated with cells at the leading edges of the systems with broader divergence areas to the rear associated with decaying cells and anvil precipitation. *Zipser et al.* [1981] constructed a schematic model of the September 14

mesoscale precipitation feature (Figure 25). The similarity of the airflow to that of a squall line system (Figures 16 and 19) is evident.

d. The mesoscale wind field near nonsquall clusters. The similarity of the air motions in nonsquall and squall clusters is
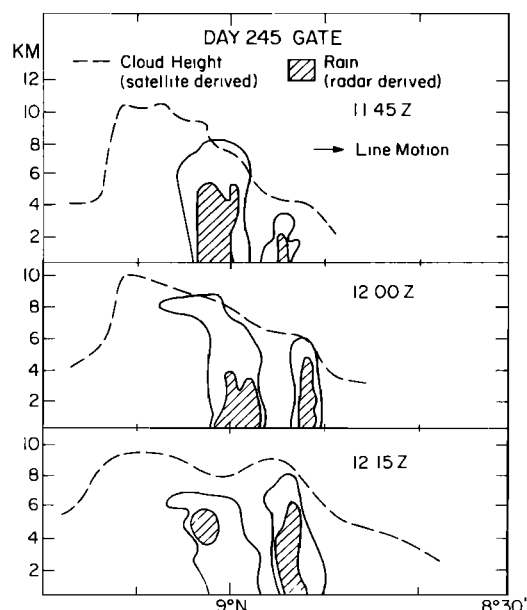
Fig. 23. Cross sections through the convective line along the aircraft flight tracks (north-south on 22°51'W) on September 2, 1974, showing sequential growth of new cells on the leading edge of a mesoscale precipitation feature. (Reprinted with permission of *Mower et al.* [1979] and the Canadian Meteorological and Oceanic Society.)

further seen in analyses of the wind fields in the vicinities of the clusters. A prominent characteristic of a squall cluster is the location of its leading line of convective cells within a zone of locally enhanced convergence. Though the MPF's of nonsquall clusters do not always exhibit linear shapes and though they may occur in various environmental flows (for example, tropical depressions, ITCZ patterns, and monsoon flows), the convectively active portions of these features can nearly always be associated with a mesoscale convergent perturbation of the low-level flow in which they are embedded.

For example, *Leary* [1979] found that in the early stages of the large September 5 nonsquall cluster, when it was dominated by mesoscale precipitation features in their formative, intensifying, and early mature stages of development, the confluent asymptote of the ITCZ became intensified about the cluster at low levels. Rather similarly, a cyclonic vortex in the surface flow formed about an intensifying mesoscale precipitation feature on September 2 [*Betts*, 1978; *Mower et al.*, 1979]. The July 15 mesoscale precipitation feature (Figure 24) coincided with a locally intensified line of confluence and convergence [*Zipser and Gautier*, 1978], and *Warner et al.* [1980] noted a tendency for the mesoscale precipitation features of September 18 to be aligned parallel to features of the low-level convergence field. A linear mesoscale precipitation feature within the nonsquall ITCZ cluster of August 12 studied by *Ogura et al.* [1979] was shown by objective analysis of GATE wind data to lie within an elongated region of enhanced convergence, which intensified as the precipitation feature and its associated upper level cloud expanded.

Late in the lifetime of the September 5 cloud cluster, when it was dominated by mesoscale precipitation features in their late mature and dissipating stages, the winds at 700 mbar formed a closed convergent cyclonic flow centered on the cluster [*Leary*, 1979], while at 200 mbar a center of divergent anticyclonic outflow developed [*Suchman and Martin*, 1976; *Leary*, 1979; *Sikdar and Hentz*, 1980]. Developments in the

700-mbar and 200-mbar flows similar to those of September 5 also occurred in the vicinity of GATE squall clusters [*Houze*, 1977; *Fortune*, 1980] and are apparently associated with the development of mesoscale ascent in deep, extensive precipitating anvil clouds characteristic of the late stages of both squall and nonsquall mesoscale precipitation features (Figures 14, 16, 19, and 25). *Frank* [1978], *Betts* [1978], *Ogura et al.* [1979], and *Sikdar and Hentz* [1980] have shown that large-scale upward motion computed from GATE wind data for occasions when cloud clusters were within the ship array increased and became a maximum in the upper troposphere (i.e., at anvil levels) during the mature stages of the clusters. During the dissipating stages the upper tropospheric upward motion remained substantial but decreased markedly in the lower troposphere, probably reflecting the mesoscale updraft-downdraft complex, although the computed vertical motion was for a bigger area than that covered by the individual clusters. The vertical motions on the scale of the clusters and anvil rain areas themselves have yet to be determined.

e. Time series of mass flux and rainfall in a mesoscale precipitation feature. *Zipser* [1980] hypothesized a time series of mass and precipitation fluxes associated with a typical (squall or nonsquall) mesoscale precipitation feature (Figure 26). It was assumed that the MPF originates 'by an imposed mesoscale convergence.' Then, '. . . the order of events is as follows: (2) rapid increase in upward convective mass flux (M_u); (3) rapid rise in rainfall, initially 100 percent convective; (4) rapid rise in mass flux in convective downdrafts $(M_d - M_{md})$; (5) gradual increase in anvil rain; (6) gradual increase in downward mass flux in mesoscale downdrafts.' The similarity of this 'typical' time series to that observed in the September 4–5 squall cluster (Figure 18) is apparent.

f. Differences between squall and nonsquall mesoscale precipitation features. At this stage of GATE research, the similarities of squall and nonsquall clusters are more evident than their differences. The main feature that sets squall systems apart from nonsquall clusters is their rapid motion, which as noted in section E1*i* may be related to the collocation of the squall systems with well-defined northeasterly or easterly jets at 600 to 700 mbar [*Frank*, 1978]. For reasons that may be rather complex, involving momentum transformations in downdrafts, or gravity wave dynamics, or both, the con-
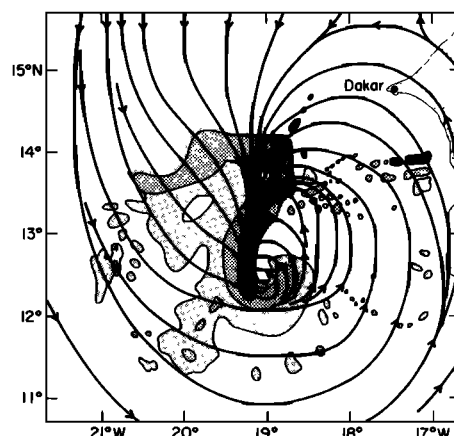

Fig. 24. Radar composite, 990-mbar streamlines superimposed, for 1400 UT, July 15, 1974. Three levels of reflectivity are indicated, determined subjectively. The northwest portion of the echo is not enclosed, as it is believed to extend beyond the limits shown. From *Zipser and Gautier* [1978].

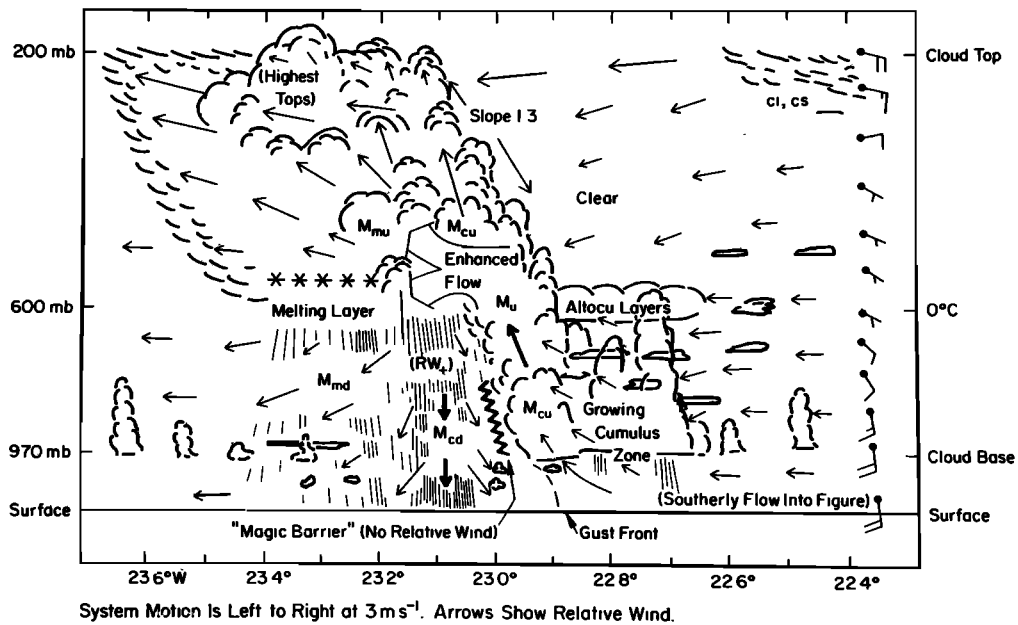System Motion Is Left to Right at 3ms⁻¹. Arrows Show Relative Wind.

Fig. 25. Schematic cross section through September 14 cloud system. From *Zipser et al.* [1981].

vection becomes organized into a line propagating with the 600- to 700-mbar flow. Nonsquall clusters apparently lack intimate connection with a 600- to 700-mbar jet.

Another difference between squall and nonsquall MPF's is that their downdrafts (both convective-scale and mesoscale) appear to be less potent than squall downdrafts in lowering the moist static energy of the lower troposphere [e.g., *Zipser and Gautier*, 1978; *Betts*, 1978; *Mower et al.*, 1979; *Zipser*, 1980]. The reason for this difference needs further study.

3. Smaller Convection Associated With Cloud Clusters

a. *Occurrence of smaller clouds in the vicinities of clus-*

ters. In discussing squall and nonsquall cloud clusters we have focused on MPF's, which, in their mature stages, constitute the type 3 and 4 (large B/C scale) radar echoes that account for most of the area covered by precipitation in cloud clusters (sections D6a and D6b). Though these B/C scale mesoscale precipitation features dominate the precipitation patterns, the log normality of the size distributions of tropical cloud and rain areas indicates the simultaneous presence of many more smaller precipitating and nonprecipitating convective clouds.

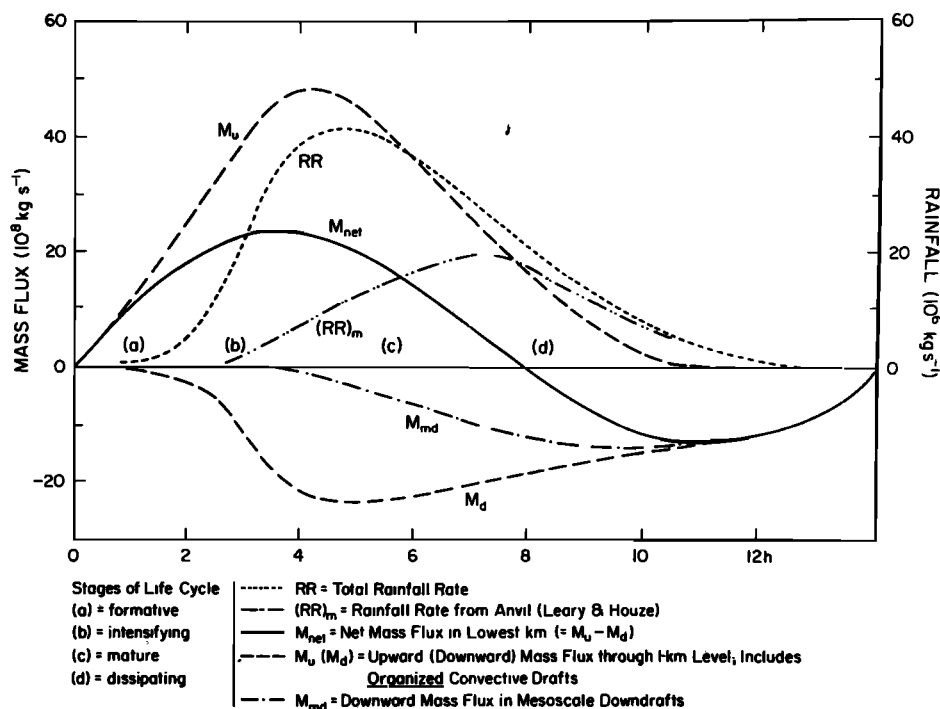b. *Cloud population associated with a cloud cluster.* *Warner et al.* [1979, 1980] have mapped the entire popu-

Fig. 26. Life cycle of typical mesoscale precipitation feature in time series. (Reprinted with permission of *Zipser* [1980].)

lation of clouds associated with the GATE nonsquall cloud cluster of September 18. Photogrammetry applied to airborne cloud photography, quantitative time lapse satellite imagery, and radar date were analyzed. The mapped clouds (Figure 27) show a gradation, with shallow nonprecipitating clouds (<2.5 km, Figure 27 (bottom)) in the southwest of the region studied giving way to deeper precipitating clouds in the northwest (Figure 27 (top)). The largest clouds (≥10 km in height) were components of MPF's located under the cirrus canopy (shown in Figure 27 (bottom)) of the cloud cluster.

c. *Types of clouds making up the population associated with the cluster.* Following *Warner et al.* [1979, 1980] and *Simpson and van Helvoirt* [1980], we may think of the clouds on September 18 in four categories, to which we assign the following terminology: (1) tiny cumulus—less than 1 km in height, nonprecipitating, (2) small cumulus—1–3 km in height, occasionally precipitating, (3) moderate cumulus—3–9 km in height, nearly always precipitating, and (4) penetrative cumulonimbus cells—over 9 km in height, always associated with precipitation, usually embedded in MPF's.

We are concerned here with the first three categories, i.e., with the tiny to moderate convective clouds. Their characteristics are discussed briefly in the following two subsections.

d. *Tiny and small cumulus.* These species differ from the deeper ones in that they do not require strong low-level convergence in order to exist. In fact, they occur over wide areas of the tropical oceans, including regions of widespread subsidence (for example, the trades), inimical to the development of the deeper clouds. These clouds arise wherever the mixed layer thickens sufficiently that moist turbulent elements can reach the condensation level. The vertical transports affected by the tiny to small cumulus maintain the moist cloud layer and typical inversion capping it against large-scale subsidence characteristic of undisturbed regions [*Betts*, 1978].

Thickening of the mixed layer and occurrence of tiny to small cumulus tend to occur within mesoscale patches, where the turbulent flux of moisture at the condensation level exceeds that at the ocean surface [*LeMone*, 1980]. (*Nicholls and LeMone* [1980] have shown that this behavior is consistent with the parametric boundary layer model of *Betts* [1976b].) *Warner et al.* [1979] found that the tiny cumulus on September 18 occurred in mesoscale patches in the forms of rows separated by 1 or 2 km and aligned along the wind shear in the manner of roll vortices [*LeMone*, 1973; *LeMone and Pennell*, 1976]. The small cumulus on September 18 described by *Warner et al.* [1979] tended, on the other hand, to occur in mesoscale patches in the forms of arcs and rings (Figure 27). In vertical cross section, the small cumulus of the arcs displayed a rather extreme slope dictated by the ambient wind shear (Figure 28).

e. *Moderate cumulus.* The moderate cumulus and penetrative cumulonimbus differ from the shallower tiny and small cumulus in two apparent respects, noted by *Simpson and van Helvoirt* [1980]:

1. The deeper clouds apparently require concentrated low-level convergence in order to be maintained, whereas the shallow clouds can exist under large-scale suppressed conditions.

2. The deeper clouds are more effective in modifying the subcloud layer by filling it with downdraft air of low moist static energy, especially when the rainfall rates are substantial [*Betts*, 1976a; *Barnes*, 1980].

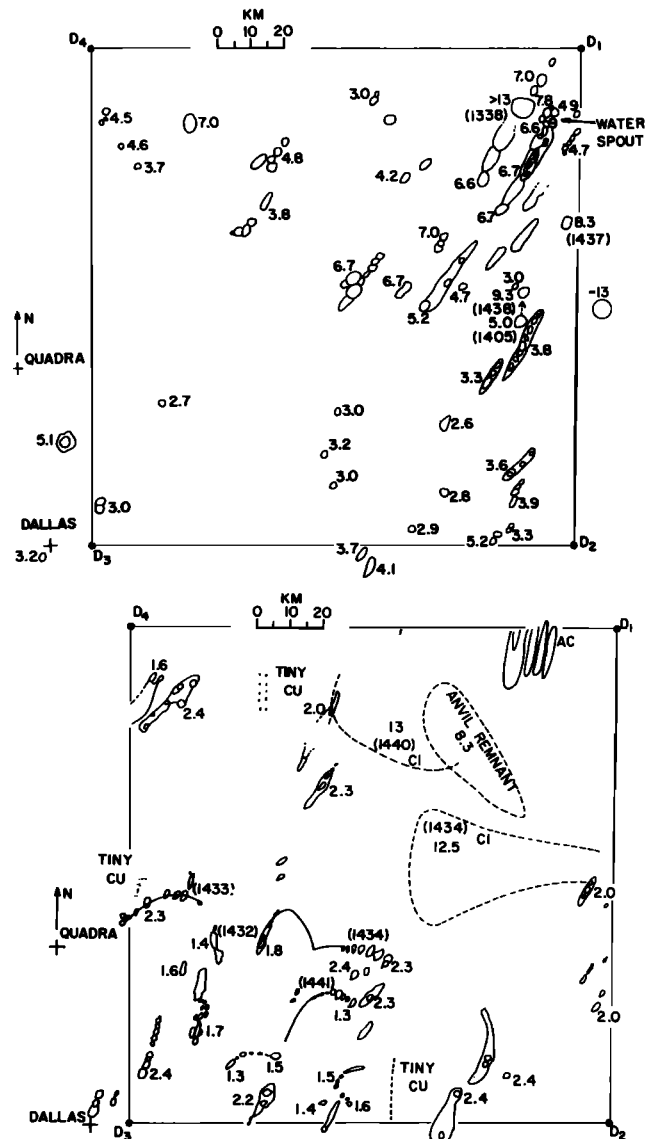In sections E1 and E2 the effects of the downdrafts of pene-

Fig. 27. Cloud map from airborne observations obtained from 1300 to 1445 UT, September 18, 1974. (Top) Active tops (outlined by contours) in the height interval 2.5–13 km. (Bottom) Clouds of height <2.5 km and anvils (dashed). Thin solid lines represent arcs of clouds. Numbers are heights (km) above the sea, and times of measurement. The corners D₁ to D₄ define the box circuit flown by the aircraft. From *Warner et al.* [1979].

trative cumulonimbus cells associated with the mesoscale precipitation features of squall and nonsquall clusters were described. In their three-dimensional cloud-model study using GATE input data from September 18, *Simpson and van Helvoirt* [1980] showed that moderate cumulus can also produce strong downdraft modification of the subcloud layer (Figure 29).

f. *Downdrafts and interactions.* The arcs of small cumulus described by *Warner et al.* [1980] appeared near precipitating clouds and were apparently triggered by outflows of dense downdraft air from regions of precipitation. As the arcs progressed through their life cycles, some of the small cumulus making up the arcs grew and became precipitating clouds, which, in turn, developed their own downdrafts that could spawn new arcs of small cumulus. This behavior of the
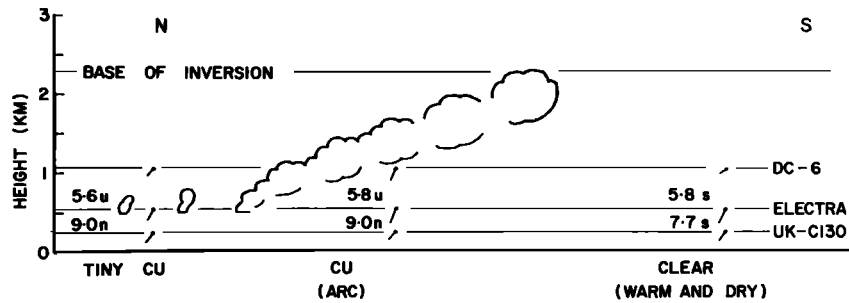
Fig. 28. Schematic cross section through a cloud arc of the type observed on September 18, 1974. The clouds were composed of a succession of thermals rising in wind shear. Numbers are temperature lapse rates (°C km^{-1}) between the levels of flight indicated, and winds are drawn as short barbs. The letter *s* means stable, *n* neutral, and *u* convectively unstable. The system moved northward (from right to left). Updrafts occurred at the clouds' leading edges, and downdrafts behind. The clear air behind the arc was warm, dry, and stably stratified, implying subsidence. From *Warner et al.* [1979].

arcs is reminiscent of the generation, on a larger scale, of new squall line systems in the vicinities of the edges of downdraft outflows of old dissipating cloud clusters (section E1a, Figure 15).

Examination of the whole spectrum of clouds associated with a cloud cluster in the intertropical convergence zone thus reveals a highly interactive assemblage in which the existence of past clouds affects the location and mesoscale spatial arrangement of future clouds. The primary mode of communication between the past and the future clouds appears to be the outflow of downdraft air from precipitating clouds. Downdraft outflows affect future cloud formation in at least two ways. First, low-level convergence becomes concentrated at the edges of the outflows, and updrafts of new clouds are triggered there. Second, the outflow of downdraft air from a precipitating cloud so completely changes the character of the planetary boundary layer [*Betts*, 1976a; *Barnes*, 1980] that wherever the outflow spreads, the formation of even tiny cumulus is prevented for hours, until the flux of latent and sensible heat from the ocean reestablishes a mixed layer of high moist static energy [*Garstang and Betts*, 1974; *Echternacht and Garstang*, 1976; *Houze*, 1977; *Zipser*, 1977; *Augstein*, 1978; *Gaynor and Mandics*, 1978]. Once reestablished, the mixed layer is ready to serve as updraft air for future clouds.

F. INTERACTION BETWEEN CONVECTION AND THE LARGE-SCALE FLOW: DIAGNOSTIC MODEL RESULTS

As noted in section B, a central objective of GATE was to estimate the bulk effects of cloud ensembles on the large-scale flow observationally. It was hoped that these estimates would help our understanding of convective parameterization models [*Rodenhuis and Betts*, 1974]. Prior to the field experiment, most of the emphasis on diagnostic modeling work was directed toward the heat and moisture transports by convection [e.g., *Yanai et al.*, 1973; *Ogura and Cho*, 1973; *Nitta*, 1975] using a cloud spectral models of the type proposed by *Ooyama* [1971] and *Arakawa and Schubert* [1974] for cumulus parameterization. Work of this type has continued with GATE data, and there has been a growing awareness of the role of transports of momentum and vorticity by clouds in the dynamics of tropical wave systems and cloud clusters. Considerable progress has been made both observationally and theoretically in understanding these transports. However, the preparation of data sets has been a major task facing researchers undertaking diagnostic modeling studies, and work is still in progress.

1. Preparation of Data Sets

a. Upper air data. Early studies have been compiled using preliminary upper air data sets [*Reed et al.*, 1977] and the A/B ship data alone [*Nitta*, 1977; *Falkovich*, 1978; *Cho et al.*, 1979b]. Many subsequent papers have been based on simple field fits to the A/B and some or all of the B ship data [*Thompson et al.*, 1979; *Reeves et al.*, 1979; *Ogura et al.*, 1979; *Frank*, 1979]. The disappointing quality of B ship winds derived from navigational aid tracking systems (which were not adequately tested before the 1974 field phase) has both delayed production and considerably reduced the quality of wind data sets on the B scale. A major effort has been in progress for the past 7 years to extract wind sets with optimum time and space filtering using spectral objective analysis methods. The Phase III data set has now been completed [*Ooyama*, 1980]. It contains a wealth of information which will be the basis of further B and A/B scale studies.

b. Radar data. The data from the four shipborne digital weather radar systems (Figure 1) provide the primary GATE precipitation measurements for use in diagnostic studies involving moisture budgets. Because of the quantitative information they provide on the structure of populations of precipitating clouds, the radar measurements constitute a set of data in addition to budgets derived from upper air data against which cloud models can be tested and constrained to indicate
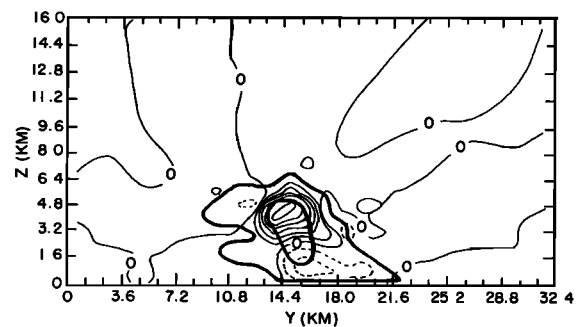

Fig. 29. Model simulation of cumulus congestus observed in GATE on September 18. The *Y* axis extends from south to north. Cloud tops at 14 km 20 min later. Primary isopleths are vertical velocities in meters per second, and contour interval is 1 m s^{-1}. Updrafts are solid; downdrafts are dashed. Heavy background isopleths are liquid water. Outer isopleth is 0 g m^{-3}; inner isopleth is 2 g m^{-3}. (Reprinted with permission of *Simpson and van Helvoirt* [1980] and Friedrich Vieweg & Sohn.)
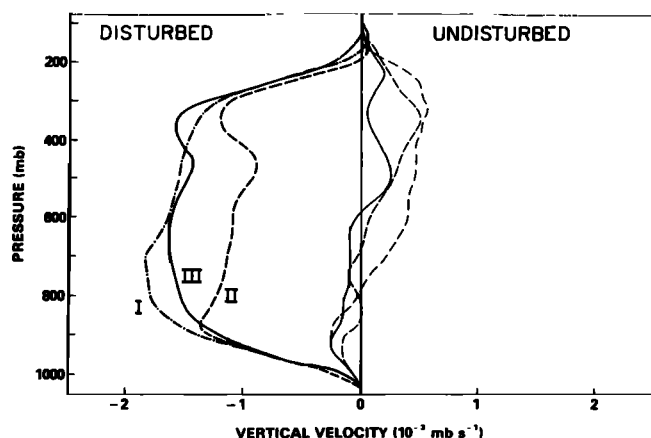
Fig. 30. Mean vertical velocity profiles for disturbed (heavy) and suppressed (light) conditions for Phase I (dashed-dotted line), Phase II (dashed), and Phase III (solid). From *Reeves et al.* [1979].

the properties of ensembles of GATE clouds [*Houze et al.*, 1980].

Preparation of the radar data for quantitative diagnostic purposes has also been a lengthy and complex effort involving radar calibrations, studies of the accuracy of functions relating power measurements to rainfall rates, intercomparisons of radars, comparisons of radar data with shipboard rain gage measurements, and studies of raindrop size distributions. As a result of careful planning and testing for several years prior to 1974 and 5 years of major effort in processing the data after GATE, the desired quantitative radar set has been produced [*Hudlow*, 1979; *Hudlow et al.*, 1980].

c. Aircraft data. Quantitative budget studies based on GATE aircraft data have had to await the enormous undertaking of processing the data from over 400 flights by several aircraft, each carrying diverse and unique instrumentation. These data are now in a form which allows such studies to be attempted, and initial work is under way (E. J. Zipser, personal communication, 1980).

2. Important Budget Study Results

Budget studies have confirmed the close coupling of deep convection and large-scale mean vertical motion ($\bar{w}$). Figure 30 [*Reeves et al.*, 1979] shows that for the three phases of GATE, deep tropospheric ascent was present only in disturbed deep convective conditions (see also *Falkovich* [1979] and *Cheng and Houze* [1979]). *Thompson et al.* [1979], *Frank* [1979], *Rodenhuis et al.* [1980], and *Ruprecht* [1980] show the close agreement between observed precipitation and precipitation derived by the budget method, in which the terms involving $\bar{w}$ dominate (Figure 31). It is thus clear that provided $\bar{w}$ can be predicted, a reasonable parameterization of rain is possible. The vertical distribution of condensation heating and water vapor modification is more difficult to obtain, since it requires a cloud transport model (section F3).

The divergence and heating profiles in the GATE area are more complex than shown by earlier studies in the tropical Pacific (Figures 32 and 33) [*Thompson et al.*, 1979]. The mean GATE divergence structure is the result of averaging various phenomena (ITCZ, wave, diurnal, cloud cluster), which each have divergence structures that are variable in time and space. The resulting complex mean profile shows low-level convergence stronger and shallower in the GATE area than in the

Pacific, with mid-tropospheric divergence and convergence below upper level divergent outflow.

Although the vorticity structures in the east Atlantic are also markedly different from those of the Pacific, exact comparisons are difficult, since the GATE data set is subject to less averaging in time and space. Low-level mean vorticity values are typically smaller or no larger than low-level divergence [*Frank*, 1978; *Reeves et al.*, 1979], indicating that the circulation is not frictionally driven as was speculated in the early planning of GATE. Furthermore, convection acts to oppose the tendency for amplification of a low-level vortex driven by convergence in a region of cyclonic vorticity (see section F3b).

3. Diagnostic Studies of Convective Transports

While the preparation of better data sets has been in progress, a considerable number of diagnostic studies of mass, thermodynamic, and vorticity transports by GATE convection have been undertaken using preliminary data. This work has been dominated by two themes: (1) the development of improved diagnostic models to interpret the data sets and the derived parameters used to characterize a convective field and (2) the need to reconcile descriptive studies (sections D and E), which indicate that transports occur on various subsynoptic scales, with the limited information in observed budget data and the highly constrained requirements of a closed parameterization theory. It is here that much work remains to be done.

a. Development of improved diagnostic models for thermodynamic transports. The diagnostic studies that have been undertaken with GATE data (see review by *Johnson* [1980a]) have been carried out in the framework of a large-scale budget equation (for heat, moisture, momentum, or vorticity) in which a residual term represents the vertical convergence of fluxes by vertical motions (presumably associated with clouds) that are unresolved by the available sounding network. A population of model clouds is then constrained to match these residual terms. The model cloud properties required to match the residual are then manipulated to decompose the residual term into physically meaningful components (for example, detrainment or compensating downward motion effects) and to relate the residual to bulk or spectral profiles of cloud vertical transports of mass, heat, moisture, or other quantities. This
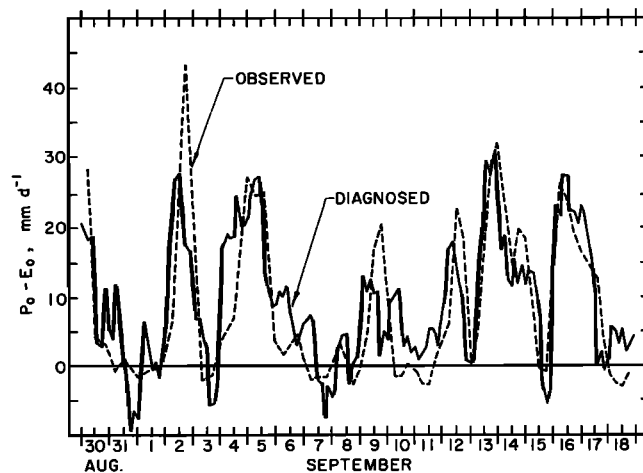

Fig. 31. Time series for Phase III of diagnosed (solid) and observed (dashed) precipitation minus evaporation. From *Thompson et al.* [1979].
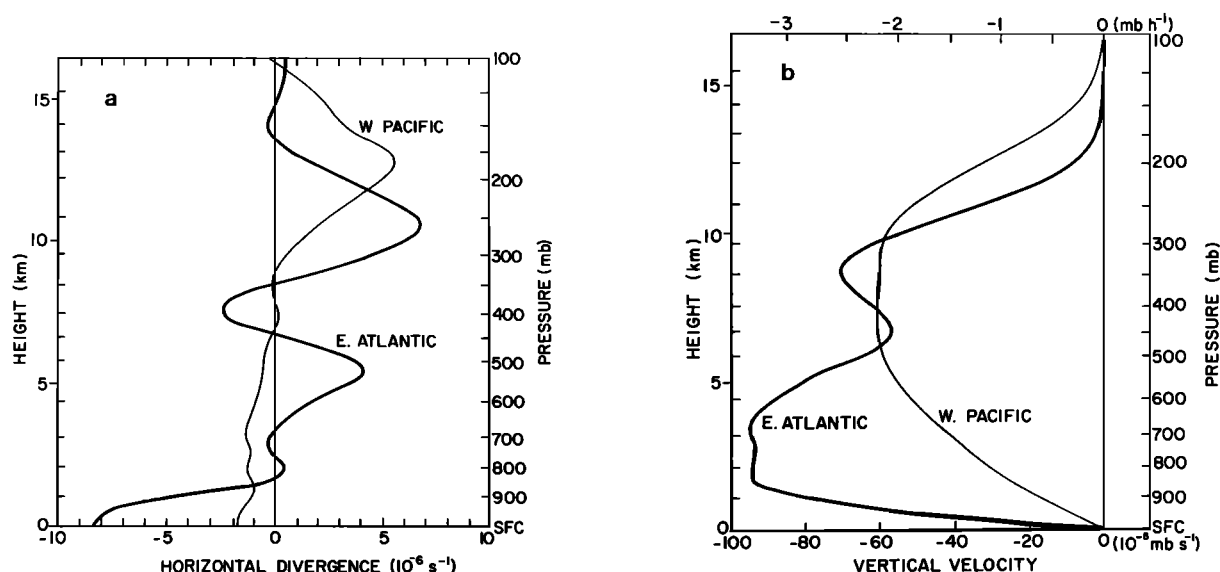
Fig. 32. Variation with height of (a) mean horizontal divergence and (b) mean vertical velocity, dp/dt, where p is pressure, for the B scale area and the west Pacific station triangle. From *Thompson et al.* [1979].

approach is relevant to parameterization of convection in large-scale numerical models, since there the objective is also to represent the residual terms in a proper way. The difficulty with the diagnostic studies is that real clouds are not simple. As shown by descriptive studies, they contain convective-scale updrafts and downdrafts, they have important entrainment and detrainment effects, they have mesoscale anvil circulations, and they are controlled not only by the resolved synoptic-scale motion field but by mesoscale convergence patterns, downdraft outflows, and probably other unresolved features. The diagnostic studies to date have emphasized determining the extent to which these various features of GATE clouds can affect convective transports.

One major area of research has been the extension of the cloud spectral approach [*Ooyama*, 1971; *Arakawa and Schubert*, 1974; *Ogura and Cho*, 1973; *Nitta*, 1975; *Yanai et al.*, 1976] to include convective downdrafts and mesoscale anvil air motions, since GATE descriptive studies have shown their importance (Figure 34, from *Houze et al.* [1980]).

In deriving cloud ensemble fluxes from synoptic data, *Johnson* [1976, 1978, 1980b] has used a spectral convective downdraft, and in the latter paper a mesoscale downdraft as well, both related to the updraft mass flux by coefficients of proportionality. An optimum value for the convective downdraft amplitude coefficient is found from matching diagnosed and observed rainfall, since the greater the evaporation associated with increased downdraft mass flux, the smaller the net precipitation. The author suggests that the amplitude of the mesoscale downdraft can be estimated by making plausible assumptions about the environmental mass flux between mesosystems. The main effect of the inclusion of more downdraft processes is to bring the net cloud mass flux closer to $\bar{w}$, particularly at low levels (Figure 35, from *Johnson* [1980b]).

Houze et al. [1980] extended their earlier work [*Houze and Leary*, 1976] in comparing diagnosed cloud ensemble fluxes computed from synoptic data by the residual method and from radar echo population data [*Austin and Houze*, 1973]. *Ruprecht* [1980] has taken a similar approach. *Houze et al.* [1980] compared GATE Phase III diagnostic results computed

by the method of *Johnson* [1976] with results based on their own radar population studies [*Cheng and Houze*, 1979]. With common model assumptions they found reasonable agreement between the mass fluxes (Figure 36) (and hence the derived heat fluxes) using these synoptic and radar approaches. They concluded that both methods were basically sound, although both gave results that depended strongly on model assumptions. *Cheng and Houze* [1980] then examined the sensitivity of the convective-scale fluxes predicted from radar data to some of these model assumptions and suggested an optimum set based on plausibility arguments. *Leary and Houze* [1980] showed that the inclusion of mesoscale anvil updrafts and downdrafts consistent with descriptive studies of GATE cloud clusters made major changes to the model-derived profiles of convective mass and heat transports.

The drawback of these increasingly complex spectral convective-scale and mesoscale models is that although these models contain terms for many of the processes now known to exist in nature, they contain several parameters and coefficients that are not readily determined from the data and must be specified. *Betts* [1975] pointed out that there are two independent budget equations. Earlier papers focused on the moist static energy transport, and models discussed above still do not use all the information in the second budget equation. *Nitta* [1977] and *Cho* [1977], on the other hand, have taken different approaches, both using the information of two budget equations to determine two unique parameters.

Nitta [1977] used the fluxes of moist static energy and the combined flux of static energy and liquid water. This does, however, require a rain parameterization. *Cho* [1977] and *Cho et al.* [1979a], extending earlier work of *Fraser* [1968], *Haman* [1969], *Betts* [1973a], and *Fraedrich* [1973], determined a combined (net) updraft and downdraft convective mass flux from the flux of static energy and liquid water, and then a second parameter from the moisture budget: a vertical profile of a time scale for recycling of air by cumulus cloud life cycles (Figure 37). Almost by design, this method gives a cumulus mass flux very close to the mean $\bar{w}$. The elegance of this theory lies in not attempting to separate updraft and downdraft
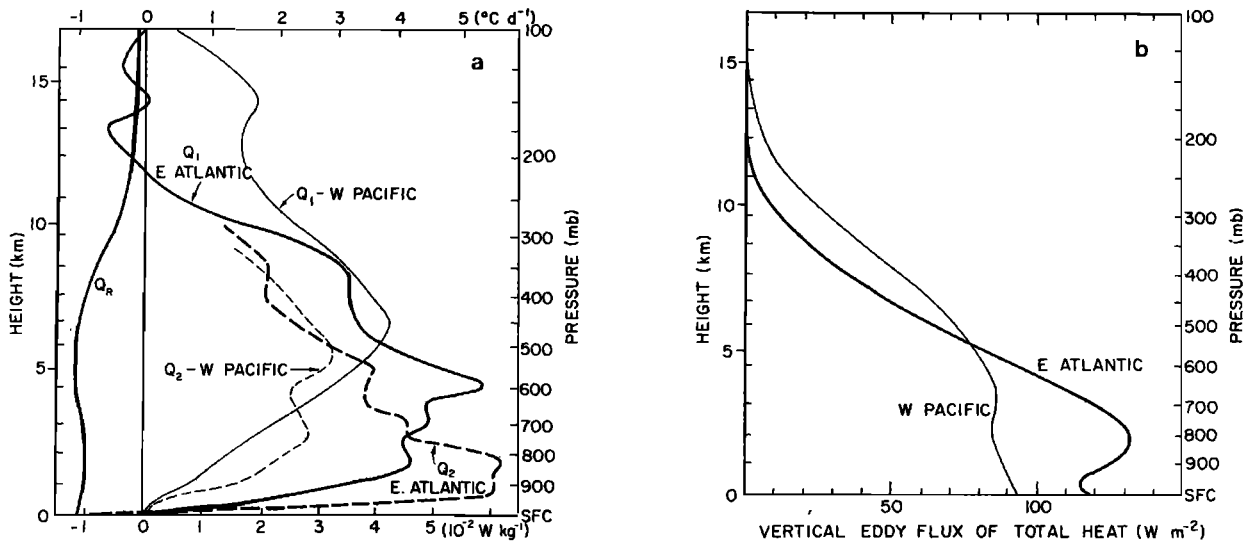
Fig. 33. Variation with height of the apparent sensible heat source Q_1 and apparent latent heat sink Q_2 and (a) the mean radiational heating Q_R and (b) the vertical eddy flux of moist static energy for the B scale area and the west Pacific triangle. From *Thompson et al.* [1979].

components. However, the recycling rate is hard to interpret, and it can only be separated from cloud moisture parameters by further assumptions (Cho assumed that detrained cloudy air is just saturated), which do not appear to be justified for deep convective ensembles, where the dominant detrainment at upper levels is updraft air and at lower levels is unsaturated downdraft air, which the theory in its present form does not separate.

It does seem, however, that further development of the diagnostic theory for deep convection is possible by combining the ideas of *Betts* [1975], *Nitta* [1977], and *Cho* [1977]. Work on this is in progress.

A different aspect of diagnostic models, which has presented some problems, is the transience of cloud systems. On the easterly wave scale, cloud storage terms associated with the changing cloud fields (which synoptic data do not resolve) are relatively small [*Johnson*, 1980b], but for the life cycle of individual cloud clusters, there seem to be significant lags between, for example, synoptic water vapor convergence and precipitation [*Betts*, 1978; *Frank*, 1979]. Whether this reflects

partly unresolved data problems or storage in a changing cloud field is not clear.

Despite their limitations, some of the diagnostic models have been applied to GATE heat and moisture budget data for GATE easterly waves [e.g., *Johnson*, 1978, 1980b; *Nitta*, 1978]. Nitta's and Johnson's results show that depending on the moisture stratification, the occurrence of convection and its associated warming and drying of the environment lag the strongest synoptic-scale low-level convergence by as much as half a day, raising questions about the applicability of conditional instability of the second kind (CISK). Their results illustrate how the vertical mass flux in deep convection is controlled by wave phase and indicate that during outbreaks of deep convection, the vertical mass flux in shallow convection is suppressed, apparently by downdrafts.

b. *Dynamic transports by cloud ensembles.* Some progress has been made in understanding the contribution of clouds to the large-scale vorticity budget [*Shapiro*, 1978; *Stevens*, 1979; *Cho et al.*, 1979b; *Reeves et al.*, 1979; *Cheng et al.*, 1980; *Cho and Cheng*, 1980; *Shapiro and Stevens*, 1980]. The observed
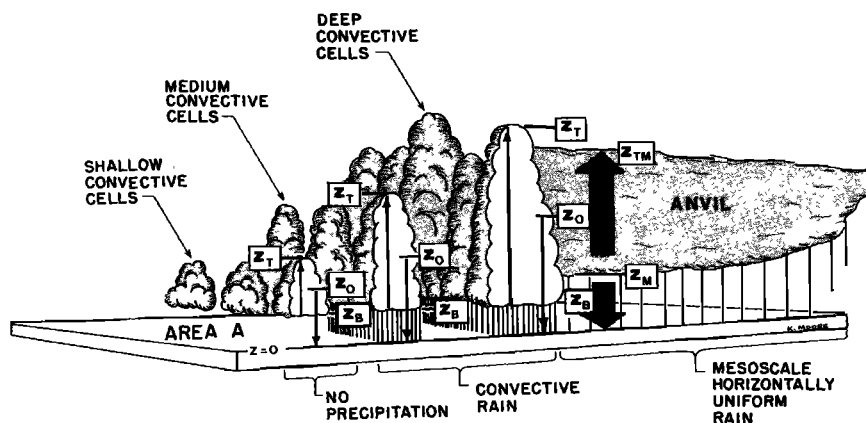

Fig. 34. Schematic of a typical population of clouds over a tropical ocean. Thin arrows represent convective scale updrafts and downdrafts. Wide arrows denote mesoscale updrafts and downdrafts. Other details and symbols for model parameters are described by *Houze et al.* [1980].
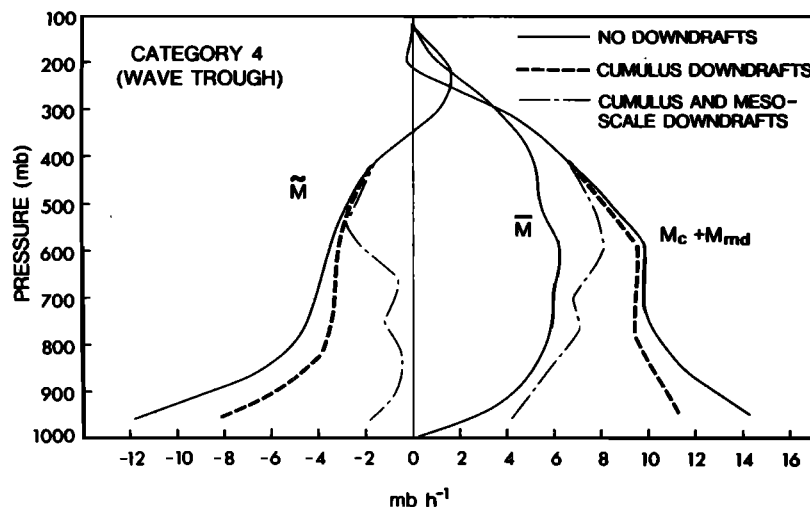
Fig. 35. Environmental mass flux $\tilde{M}$, mean mass flux $\bar{M}$, and net convective mass flux $M_c + M_{md}$ for wave trough for case with and without downdrafts. From *Johnson* [1980b].

vorticity source residuals are complex (as are the divergence profiles) but generally show that at low levels, the convection acts as a sink of vorticity which opposes the amplification that low-level convergence in a region of positive vorticity would produce [e.g., *Reeves et al.* 1979]. This is of great dynamic significance and seems consistent with the observation that very few GATE systems showed signs of low-level vorticity amplification. There are some indicators of a similar effect at high levels—of a convective source opposing anticyclonic amplification—but different diagnostic studies are not consistent, or show both sources and sinks in the upper troposphere. The higher-resolution fields of K. Ooyama (unpublished manuscript, 1980) show fascinating upper level vorticity structure, which clearly needs further study (Figure 38).

Reeves et al. [1979] present phase-average vorticity budget computations and a disturbed-suppressed stratification (Figure 39), which show the increased vorticity sink at low levels during the disturbed periods mentioned above. The budgets also show a mid-tropospheric positive vorticity source during undisturbed conditions, which could be associated with shallow to mid-level convection. However, both disturbed and suppressed budgets show a similar vorticity source at 200 mbar whose origin is unclear.

Cho et al. [1979b] and *Cho and Cheng* [1980] develop a theoretical basis for modeling vorticity transports by clouds using a continuous transient model for a cumulus cloud based on that of *Cho* [1977]. They show the importance of horizontal transports of vorticity on the cloud scale, associated with the large vorticity couplets typically found in cumulonimbus. They also show, however, that average in-cloud vorticities are comparable to large-scale average vorticity (though somewhat larger). They find good agreement between A/B scale budget residuals and parameterized values (Figure 40). Their parameterization needs cloud boundary values of vorticity, and these they estimate from a potential vorticity budget analysis [*Cheng et al.*, 1980].

The papers by *Shapiro* [1978], *Stevens* [1979], and *Shapiro and Stevens* [1980] explore the vorticity budget of the composite easterly wave. Their parameterization of the residual, using a single bulk cloud model, gives reasonably good agreement between observed and parameterized sources but shows that spectral models are much worse because the vorticity

budget for each cloud spectral type is unrealistic. They also find problems with the diagnosis of cloud mass flux. They conclude that their model was theoretically equivalent to the transient cloud model of *Cho and Cheng* [1980].

Stevens [1979] and *Shapiro and Stevens* [1980] attempt an analysis of the momentum budget for the wave, using the data of *Thompson et al.* [1979] and computing the wave pressure field by integrating the hydrostatic equation using wave perturbation virtual temperatures. The budgets tend to show, depending on wave phase, either sources of sinks of momentum at all heights. They conclude that simple interpretations or parameterizations, which only transport momentum, were not apparent.

G. PARAMETERIZATION TESTS AND CONVECTIVE MODELING

The testing of convective parameterization theories for use in numerical models was an important GATE objective. Some of this work has been done, but much remains to be accomplished. With the realization of the importance of convective transports of vorticity and momentum [*Stevens et al.*, 1977; *Shapiro and Stevens*, 1980; *Cho and Cheng*, 1980], the large effects of clouds on the radiative divergence profile [*Cox and Griffith*, 1979], and the importance of mesoscale anvil circulations [*Johnson*, 1980b; *Leary and Houze*, 1980] the problem has become a much larger one. The debate continues over
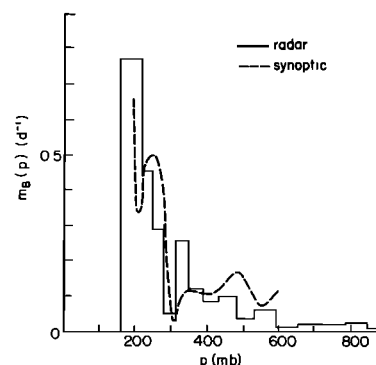

Fig. 36. Cell base mass transport spectrum diagnosed by the radar and synoptic approaches. From *Houze et al.* [1980].
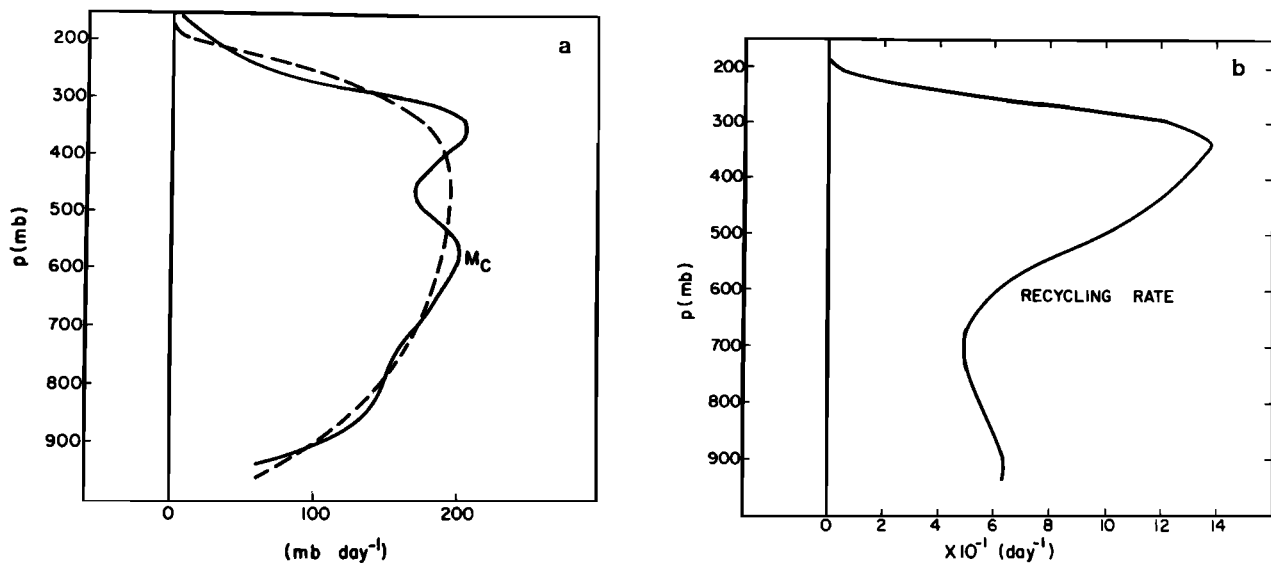
Fig. 37. (a) GATE A/B scale total cloud mass flux M_c and (b) recycling rate by cumulus clouds for the period 0000–2400, September 2, 1974. Dashed M_c curve is smoothed profile. From *Cheng et al.* [1980].

whether all convective systems (including, for example, the squall line) are parameterizable and whether in hurricane modeling it is necessary or desirable to parameterize convection. *Rosenthal* [1979] shows the extreme sensitivity of an axisymmetric hurricane model to different convective parameterizations. He further finds, using horizontal grids of 10–20 km, which are sufficient to resolve mesoscale cloud structures but not individual convective towers, that latent heat release on the resolvable scale is in some cases responsible for storm amplification. *Rosenthal* [1978, 1980] shows a hurricane simulation in which only latent heat release on the resolvable scales is included. The initial stages of the simulation show a squall-type mesoscale cloud structure that propagates in apparent independence of the vortex-scale flow, which shows no significant amplification. It is only later in the simulation with nonsquall cloud structure that cooperative development of the CISK type takes place.

1. Large-Scale Numerical Modeling

The testing of parameterization schemes is inherent in large-scale numerical model simulations. Recently, *Slingo* [1980] has reported on a coupled cloud-radiation parameterization used in the British 11-layer tropical model and tested on GATE data. Layer clouds at low, middle, and high levels are determined statistically from large-scale relative humidity and, for the low-level clouds (mainly stratocumulus under inversions), from lapse rate. Deep convection is predicted using the parameterization of *Lyne and Rowntree* [1976]. Tests show realistic distributions of stratocumulus off Africa and South America and upper and middle level layer clouds developing in the vicinity of deep convection in a manner somewhat reminiscent of the anvil cloud development seen in case studies (sections E and F). Other work has been done by *Krishna-murti et al.* [1979, 1980] and *Miyakoda and Sirutis* [1977].

2. Semiprognostic Tests

Semiprognostic tests involve computing the fluxes by an ensemble of convection in a region of space and period of time representative of a grid volume and time step of a large-scale numerical model and comparing the results with observations. *Lord* [1978] and *Krishnamurti et al.* [1980] have carried out

such tests on GATE Phase III data with the ensemble fluxes computed by several parametric schemes, including hard and soft convective adjustment, *Arakawa and Schubert*'s [1974] scheme, and *Kuo*'s [1965, 1974] schemes. *Krishnamurti et al.* show that hard convective adjustment gives massive rainfall at the first time step, with a consequent radical change in the atmospheric thermal and moisture structure.

Soft convective adjustment, which only adjusts over a fraction of the grid, can give reasonable mean rainfall rates for the entire period but poor day-by-day agreement. *Kuo*'s [1965] scheme, which partitions the moisture convergence, under-predicts rainfall but has good phase agreement. *Kuo*'s [1974] scheme and the *Arakawa and Schubert* [1974] scheme (tested by both *Lord* [1978] and *Krishnamurti et al.* [1980]) both give excellent agreement between observed and predicted precipitation (Figure 41). *Krishnamurti et al.* found that the rainfall

Fig. 38. Relative vorticity field at 227 mbar at 1800 UT, September 5, 1974, showing cyclonic (solid lines) and anticyclonic (dashed lines) vorticity couplet (units: 10^{-6} s^{-1}) across strongly divergent outflow over cloud cluster complex. The domain is centered on the A/B ship array (dotted). The ordinate and abscissa are latitude and longitude in degrees. The wind barbs are conventional (single long barb equals 10 knots (5 m s^{-1})). From K. Ooyama (unpublished manuscript, 1980).

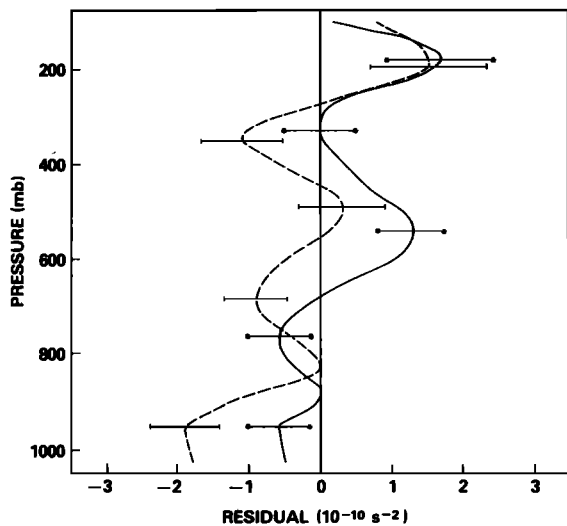Fig. 39. Mean apparent vorticity source including friction and subgrid scale processes only for disturbed (dashed) and undisturbed (solid) conditions with confidence intervals indicated by bars. From *Reeves et al.* [1979].

agreed very closely with the vertical advection of water vapor. Lord's work, however, shows that a successful precipitation comparison is not a sufficient test of the parameterization scheme's ability to reproduce realistic profiles of warming and drying of the environment by the convective fluxes.

Soong and Tao [1980] carried out semiprognostic tests on GATE data with a two-dimensional cloud ensemble model developed by *Soong and Ogura* [1980]. Domain-averaged vertical and horizontal wind and initial thermodynamic structure were prescribed for an observed deep convective situation. A randomly generated population of model clouds was allowed to develop for 6 hours within a domain 64 km in horizontal dimension. Fluxes by the model clouds produced profiles of warming and drying over the model domain that compared favorably with observed profiles. *Kuo's* [1965] parameterization scheme gave a less favorable comparison.

3. Shallow Cumulus and Stratocumulus Modeling

Although the modeling and parametric work described in this section has not been done using GATE data, much of it is relevant to GATE objectives and will be used for further analyses. Work has been done on the construction of parametric models for shallow cumulus layers [*Albrecht et al.*, 1979; *Albrecht*, 1979]. These papers discuss the evolution of a mixed layer type model [*Betts*, 1973a] for the trade wind boundary layer and show good agreement for atmospheric structure and convective fluxes with values observed during the Atlantic Tradewind Experiment (1969). This model was also used to simulate diurnal variations and showed in the limiting case of a stratocumulus layer good agreement with *Schubert* [1976]. *Schubert* [1976] and *Schubert et al.* [1979a, b] extend *Lilly's* [1968] stratocumulus model and apply it to regions of horizontally inhomogenous sea-surface temperature and large-scale divergence. There has been considerable discussion of the appropriate parameterization of radiation for stratocumulus: specifically, the degree to which radiative cooling can be regarded as part of a cloud top boundary condition, or a mechanism for the generation of turbulence in the cloud layer [*Deardorff*, 1976; *Kahn and Businger*, 1979; *Lilly and Schubert*, 1980; *Deardorff and Businger*, 1980; *Randall*, 1980a]. *Slingo's* [1980] cloud parameterization (section G1) includes stratocumulus with radiative feedback. The breakup of a stratocumulus layer through cloud top entrainment instability has been modeled by *Randall* [1980b] and *Deardorff* [1980]. The three-dimensional modeling of shallow cumulus populations has advanced considerably [*Sommeria*, 1976; *Sommeria and LeMone*, 1978]. In the latter paper the authors compare model parameters with experimental data and find good agreement for some parameters. Subsequently, *Beniston and Sommeria* [1981] used the three-dimensional model to test hypotheses of the parametric models of *Yanai et al.* [1973], *Betts* [1975, 1976b], and *Fraedrich* [1976]. They showed that the coupling of the convective thermodynamic fluxes through a bulk convective mass flux is a very accurate parameterization. They also confirmed the usefulness of the coupling of the cloud and
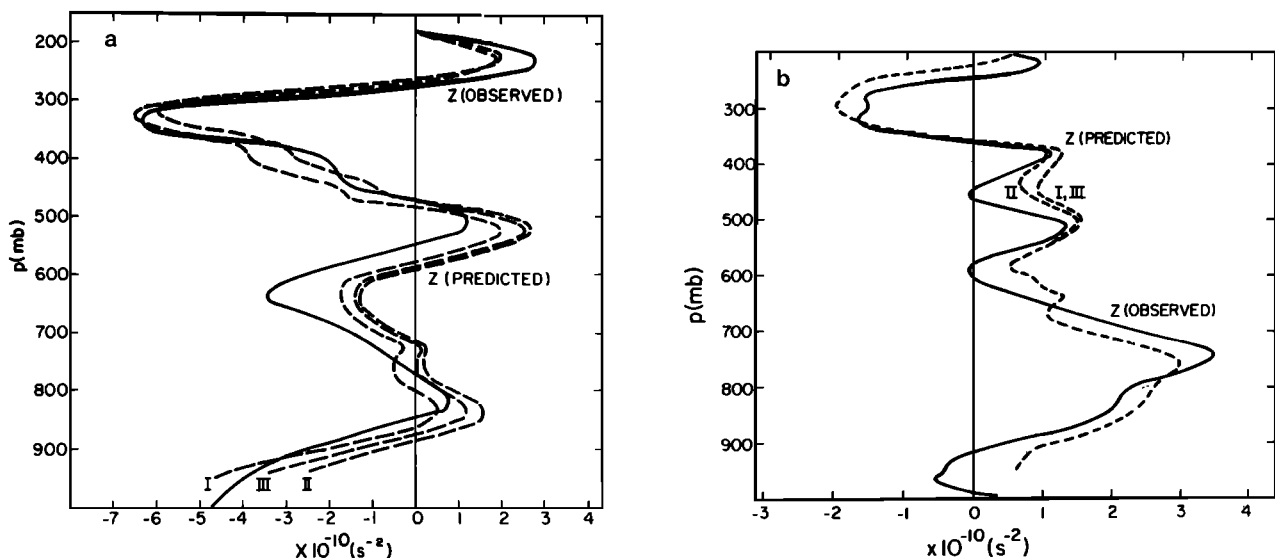

Fig. 40. Comparison between the observed (solid) and predicted (dashed) apparent vorticity sources for (a) September 2 and (b) September 9, 1974. Three different predicted sources are shown for different cloud-scale vorticity parameterizations. From *Cho and Cheng* [1980].
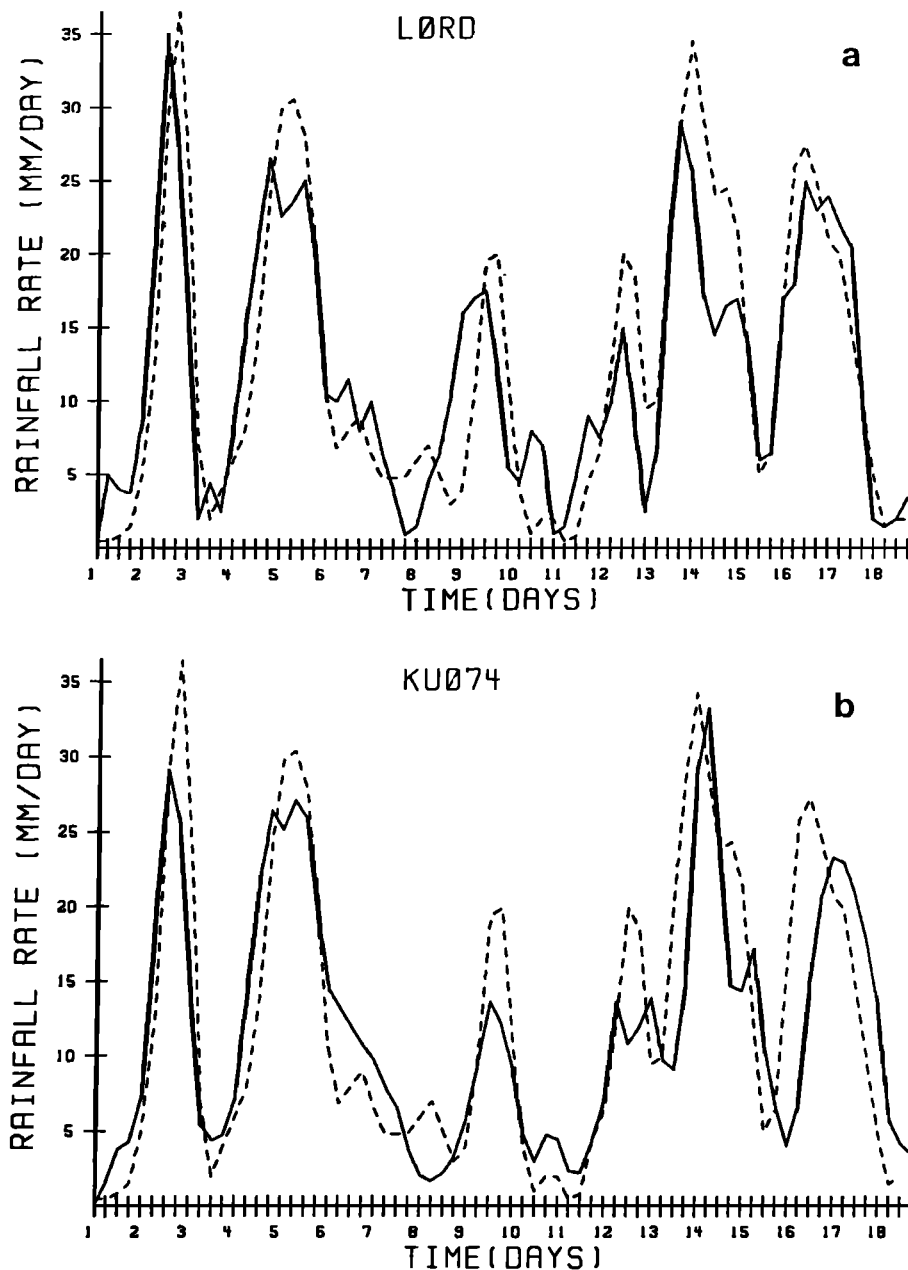
Fig. 41. Comparison between observed (dashed line) and predicted (solid line) rainfall rates (mm day^{-1}) for September 1-18, 1974, using (a) Lord's [1978] scheme and (b) Kuo's [1974] scheme. From Krishnamurti et al. [1980].

subcloud layers using two closure parameters, as proposed by Betts [1976b]. The comparison with Fraedrich's [1976] cloud population parameterization scheme is less satisfactory. The model cloud population (whose realism is admittedly questionable) differs appreciably from the simple exponential distribution proposed by Fraedrich, with corresponding differences in the mass flux distributions.

H. CONCLUSIONS

Convection that occurs in the region of planetary-scale lifting associated with the tropical Hadley cells was documented extensively in GATE by upper air soundings, satellite, meteorological radar, and instrumented aircraft. Though much of

the data have yet to be analyzed, many aspects of the structure of the convection and its relation to larger-scale flow have been revealed by detailed studies of a few examples of GATE convective systems, by limited or preliminary studies of a somewhat larger number of systems, and by statistical overviews of the satellite, radar, and aircraft data.

As had been hoped for in the planning of GATE, the convection sampled in the experiment resided in the center of the zone of ITCZ cloudiness extending across the eastern equatorial Atlantic Ocean, and as had been anticipated, the convection was dominated by cloud clusters. The frequency of clusters in time and space was modulated by synoptic-scale easterly waves and diurnal cycles of radiative heating and cooling.

The cloud clusters were of two types: squall clusters, which propagated rapidly and were associated with pronounced vertical wind shear, and nonsquall clusters, which propagated slowly and were associated with weaker wind shear.

Cloud clusters were characterized by large upper level cloud shields that emanated from penetrative cumulonimbus. Accompanying the deep cumulonimbus was a spectrum of smaller convective features ranging from moderate cumulonimbus down to tiny nonprecipitating cumulus. The spectrum of sizes of these convective features, whether measured in terms of height, area, duration, or rainfall rate, was log normal. That is, there existed a great many smaller convective clouds and rain areas for each large cumulonimbus rain area in a cloud cluster.

However, the relatively few large cumulonimbus rain areas, referred to as 'mesoscale precipitation features,' accounted for about 90% of the rain in GATE. These mesoscale precipitation features were the preferred regions where the deepest convective cells or 'hot towers,' hypothesized to exist by *Riehl and Malkus* [1958], actually formed and penetrated to the tropopause.

As a mesoscale precipitation feature matured, it developed a region of stratiform precipitation adjacent to its active cells. The stratiform portion of the feature consisted partly of older decayed cells and, in important cases, occupied the majority of the area covered by the mesoscale precipitation feature. A large fraction of the total rainfall in GATE fell as stratiform precipitation of this type. The stratiform precipitation fell from the middle level base of the anvil cloud shield that interconnected the various mesoscale precipitation features of a cloud cluster. Associated with the stratiform precipitation below the base of the anvil was a mesoscale (as opposed to cumulus-scale) downdraft similar to that described by *Zipser* [1969]. This downdraft originated at about the 0°C level, and the air in it was generally unsaturated and cooled by melting and evaporation of the falling precipitation. A mesoscale region of ascent appeared to exist within the anvil cloud itself, above the mesoscale downdraft. The existence of the mesoscale updraft needs to be confirmed. However, both it and the mesoscale downdraft are consistent with the observation of large-scale convergence in the middle troposphere and divergence at the surface and at high levels in regions containing clusters that are in middle to late stages of development.

In the dissipating stage of a mesoscale precipitation feature, the convective cells become less numerous and weaker, and the stratiform precipitation dominates the feature.

The downdrafts, both cumulus-scale and mesoscale, from a mesoscale precipitation feature invade the planetary boundary layer and fill it with air of low moist static energy. Moderate cumulonimbus, existing as part of the spectrum of smaller convective features associated with clusters, also produce significant downdraft modification of the subcloud layer. As downdraft air spreads out in the boundary layer, it influences the patterns of new cloud formation. New clouds are suppressed everywhere within the downdraft-covered region; however, both small cumuli and incipient major clusters tend to form at the edges of the downdraft air, where low-level convergence becomes enhanced. Thus cloud patterns are controlled not only by large-scale phenomena such as the Hadley cells, synoptic-scale waves, and diurnal radiative cycles, but also by the existence of past clouds, the medium of communication between the past and present clouds being the downdrafts.

Representing tropical clouds in a mathematically suitable way for including their effects in numerical models of large-scale flow remains an objective of GATE research. The descriptive and statistical studies of GATE convective systems have led to the realization that a variety of physical processes must be accounted for in such models. Besides cumulus-scale updrafts, it now appears that cumulus-scale downdrafts, mesoscale downdrafts, mesoscale updrafts, downdraft-induced boundary layer transformations, and radiative feedbacks are all important in modifying the thermodynamic and dynamic structure of the large-scale environment. That controls over new convective cloud formation are not purely large scale but involve the history of past clouds and that feedbacks to the environment may not be directly from convective to synoptic scale but involve the generation of intermediate-scale disturbances are now eminently apparent and must be considered in trying to understand and model scale interactions in the tropics.

Further diagnostic and parametric studies are needed. It is clear that on large enough scales (700 km and 24 hours), precipitation amd mean vertical motion are closely coupled. This gives encouragement for the parameterization of convection. However, it has not been shown that we can predict the detailed vertical structure of the convective fluxes with sufficient accuracy. GATE, moreover, has shown that the vorticity transports by convection cannot be neglected in favor of a purely thermodynamic convective parameterization. On space and time scales more comparable to the mesoscale precipitation areas (100 km and 4 hours) we are far from understanding the parametric problem.

Much remains to be done to understand the mechanism of scale interactions in the tropics, and many GATE data remain unexamined. We anticipate that in future years these data will used to study more examples of GATE convective systems and their interactions with their environments will be intensively studied and, as a result, the mechanisms involved will be closer to being unraveled.

REFERENCES

Albrecht, B. A., A model for the thermodynamic structure of the tradewind boundary layer, II, Applications, *J. Atmos. Sci., 36*, 90–98, 1979.

Albrecht, B. A., A. K. Betts, W. H. Schubert, and S. K. Cox, A model for the thermodynamic structure of the trade-wind boundary layer, I, Theroretical formulation and sensitivity tests, *J. Atmos. Sci., 36*, 73–89, 1979.

Arakawa, A., and W. Schubert, Interaction of a cumulus cloud ensemble with the large-scale environment, I, *J. Atmos. Sci., 35*, 674–701, 1974.

Arkell, R., and M. Hudlow, *GATE International Meteorological Radar Atlas*, 222 pp., U.S. Government Printing Office, Washington, D. C., 1977.

Aspliden, C. I., Y. Tourre, and J. C. Sabine, Some climatological aspects of West African disturbance lines during GATE, *Mon. Weather Rev., 104*, 1029–1035, 1976.

Augstein, E., The atmospheric boundary layer over the tropical oceans, in *Meteorology Over the Tropical Oceans*, pp. 73–103, Royal Meteorological Society, Bracknell, England, 1978.

Austin, P. M., and S. G. Geotis, Raindrop sizes and related parameters for GATE, *J. Appl. Meteorol., 18*, 569–575, 1979.

Austin, P. M., and R. A. Houze, Jr., A technique for computing vertical transports by precipitating cumuli, *J. Atmos. Sci., 30*, 1100–1111, 1973.

Ball, J. T., S. J. Thoren, and M. A. Atwater, Cloud-coverage characteristics during Phase III of GATE as derived from satellite and ship data, *Mon. Weather Rev., 108*, 1419–1429, 1980.

Barnes, G. M., Subcloud layer energetics of precipitating convection, Ph.D. dissertation, 212 pp., Univ. of Va., Charlottesville, 1980.

Beniston, M. G., and G. Sommeria, Use of a detailed planetary boundary layer model for parameterization purposes, *J. Atmos. Sci., 38*, 780–797, 1981.

Betts, A. K., Non-precipitating cumulus convection and its parameterization, *Quart. J. R. Meteorol. Soc., 99*, 178–196, 1973a.

Betts, A. K., A composite cumulonimbus budget, *J. Atmos. Sci., 30*, 597–610, 1973b.

Betts, A. K., Parametric interpretation of trade-wind cumulus budget studies, *J. Atmos. Sci., 32*, 1934–1945, 1975.

Betts, A. K., The thermodynamic transformation of the tropical subcloud layer by precipitation and downdrafts, *J. Atmos. Sci., 33*, 1008–1020, 1976a.

Betts, A. K., Modeling subcloud layer structure and interaction with a shallow cumulus layer, *J. Atmos. Sci., 33*, 2363–2382, 1976b.

Betts, A. K., Convection in the tropics, in *Meteorology Over the Tropical Oceans*, pp. 105–132, Royal Meteorological Society, Bracknell, England, 1978.

Betts, A. K., and M. F. Silva Dias, Unsaturated downdraft thermodynamics in cumulonimbus, *J. Atmos. Sci., 36*, 1061–1071, 1979.

Betts, A. K., R. W. Grover, and M. W. Moncrieff, Structure and motion of tropical squall-lines over Venezuela, *Quart. J. R. Meteorol. Soc., 102*, 395–404, 1976.

Bibikova, T. N., V. N. Kozhevnikov, E. V. Zhurba, Y. A. Romanov, and A. K. Khrgian, Some results from cloud observations in the tropics, *Sov. Meteorol. Hydrol., 8*, 67–74, 1977.

Borovikov, A. M., I. P. Mazin, V. Melnichuk, and P. Willis, Case study of analysis of individual Cb physical structure, *GATE Rep. 14*, vol. II, pp. 212–216, Int. Counc. of Sci. Unions/World Meteorol. Org., Geneva, 1975.

Borovikov, A. M., I. P. Mazin, and A. N. Nevzorov, Cloud structure peculiarities in the eastern zone of tropical Atlantic, in *Proceedings of the International Scientific Conference on the Energetics of the Tropical Atmosphere*, pp. 43–47, International Council of Scientific Unions/World Meteorological Society, Geneva, 1978.

Brown, J. M., Mesoscale unsaturated downdrafts driven by rainfall evaporation: A numerical study, *J. Atmos. Sci., 36*, 313–338, 1979.

Burpee, R. W. Some features of synoptic-scale waves based on compositing analysis of GATE data, *Mon. Weather Rev., 103*, 921–925, 1975.

Byers, H. R., and R. R. Braham, Jr., *The Thunderstorm*, 287 pp., U.S. Government Printing Office, Washington, D. C., 1949.

Cheng, C.-P., and R. A. Houze, Jr., The distribution of convective and mesoscale precipitation in GATE radar echo patterns, *Mon. Weather Rev., 107*, 1370–1381, 1979.

Cheng, C.-P., and R. A. Houze, Jr., Sensitivity of diagnosed convective fluxes to model assumptions, *J. Atmos. Sci., 37*, 774–783, 1980.

Cheng, L., T.-C. Yip, and H.-R. Cho, Determination of mean cumulus cloud voriticity from GATE A/B-scale potential vorticity budget, *J. Atmos. Sci., 37*, 797–811, 1980.

Cho, H.-R., Contribution of cumulus cloud life-cycle effects to the large-scale heat and moisture budget equations, *J. Atmos. Sci., 34*, 87–97, 1977.

Cho, H.-R., and L. Cheng, Parameterization of horizontal transport of vorticity by cumulus convection, *J. Atmos. Sci., 37*, 812–826, 1980.

Cho, H.-R., L. Cheng, and R. M. Bloxam, The representation of cumulus cloud effects in the large-scale vorticity equation, *J. Atmos. Sci., 36*, 127–139, 1979a.

Cho, H.-R., R. M. Bloxam, and L. Cheng, GATE A/B-scale budget analysis, *Atmos. Ocean, 17*, 60–76, 1979b.

Cox, S. K., and K. T. Griffith, Estimates of radiative divergence during Phase III of the GARP Atlantic Tropical Experiment, II, Analysis of Phase III results, *J. Atmos. Sci., 36*, 586–601, 1979.

Cunning, J. B., and R. I. Sax, Raindrop size distributions and Z-R relationships measured on the NOAA DC-6 and the ship Researcher within the GATE B-scale array, *NOAA Tech. Memo. ERL-WMPO-37*, 136 pp., Natl. Oceanic and Atmos. Admin., Rockville, Md., 1977a. (Available from National Technical Information Service, PB-269 659/961.)

Cunning, J. B., and R. I. Sax, A Z-R relationship for the GATE B-scalae array, *Mon. Weather Rev., 105*, 1330–1336, 1977b.

Deardorff, J. W., On the entrainment rate of a stratocumulus topped mixed layer in a strong inversion, *Quart. J. R. Meteorol. Soc., 101*, 563–582, 1976.

Deardorff, J. W., Cloud top entrainment instability, *J. Atmos. Sci., 37*, 131–147, 1980.

Deardorff, J. W., and J. A. Businger, Comments on 'Marine stratocumulus convection. Part I: Governing equations and horizontally homogeneous solutions,' *J. Atmos. Sci., 37*, 481–482, 1980.

Eldridge, R. H., A synoptic study of West African disturbance lines, *Quart. J. R. Meteorol. Soc., 83*, 303–314, 1957.

Echternacht, K. L., and M. Garstang, Changes in the structure of the tropical subcloud layer from the undisturbed to disturbed states, *Mon. Weather Rev., 104*, 407–417, 1976.

Falkovich, A. I., On the problem of energy balance in the ITCZ, in *Proceedings of the International Scientific Conference on the Energetics of the Tropical Atmosphere*, pp. 219–227, International Council of Scientific Unions/World Meteorological Organization, Geneva, 1978.

Falkovich, A. I., *Dynamics and Energetics of the ITCZ*, 247 pp., Gidrometeoizdat, Leningrad, USSR, 1979.

Fitzjarrald, D., The boundary layer over the tropical ocean, Ph.D. dissertation, 180 pp., Univ. of Va., Charlottesville, 1979.

Fortune, M., Properties of African disturbance lines inferred from time-lapse satellite imagery, *Mon. Weather Rev., 108*, 153–168, 1980.

Fraedrich, K., On the parameterization of cumulus convection by lateral mixing and compensating subsidence, *J. Atmos. Sci., 30*, 408–413, 1973.

Fraderich, K., A mass budget of an ensemble of transient cumulus clouds determined from direct cloud observations, *J. Atmos. Sci., 33*, 262–268, 1976.

Frank, N. L., Atlantic tropical systems of 1969, *Mon. Weather Rev., 98*, 307–314, 1970.

Frank, W. M., The life cycles of GATE convective systems, *J. Atmos. Sci., 35*, 1256–1264, 1978.

Frank, W. M., Individual time period analyses over the GATE ship array, *Mon. Weather Rev., 107*, 1600–1616, 1979.

Fraser, A. B., The white box: The mean mechanics of the cumulus cycle, *Quart. J. R. Meteorol. Soc., 94*, 71–87, 1968.

Fritsch, J. M., Cumulus dynamics: Local compensating subsidence and its implications for cumulus parameterization, *Pure Appl. Geophys., 113*, 851–867, 1975.

Fritsch, J. M., and C. G. Chappell, Numerical prediction of convectively driven mesoscale pressure systems, II, Mesoscale model, *J. Atmos. Sci., 37*, 1734–1762, 1980.

Garstang, M. A., and A. K. Betts, A review of the tropical boundary layer and cumulus convection: Structure, parameterization and modeling, *Bull. Am. Meteorol. Soc., 55*, 1195–1205, 1974.

Gaynor, J. E., and P. A. Mandics, Analysis of the tropical marine boundary layer during GATE using acoustic sounder data, *Mon. Weather Rev., 106*, 223–232, 1978.

Gaynor, J. E., and C. F. Ropelewski, Analysis of convectively modified GATE boundary layer using in situ and acoustic sounder data, *Mon. Weather Rev., 107*, 985–993, 1979.

Gray, W. M., Cumulus convection and larger scale circulations, I, Broadscale and mesoscale considerations, *Mon. Weather Rev., 101*, 839–855, 1973.

Gray, W. M., and R. W. Jacobson, Jr., Diurnal variation of oceanic deep cumulus convection, *Mon. Weather Rev., 105*, 1171–1188, 1977.

Griffith, C. G., W. L. Woodley, J. S. Griffin, and S. C. Stromatt, *Satellite-Derived Precipitation Atlas for GATE*, 280 pp., U.S. Department of Commerce, Washington, D. C., 1980.

Gruber, A., An estimate of the daily variation of cloudiness over the GATE A/B area, *Mon. Weather Rev., 104*, 1036–1039, 1976.

Haman, K., On the influence of convective clouds on the large-scale stratification, *Tellus, 21,* 40-53, 1969.

Hamilton, R. A., and J. W. Archbold, Meteorology of Nigeria and adjacent territory, *Quart. J. R. Meteorol. Soc., 71,* 231-262, 1945.

Holle, R. L., J. Simpson, and S. W. Leavitt, GATE B-scale cloudiness from whole-sky cameras on four U.S. ships, *Mon. Weather Rev., 107,* 874-895, 1979.

Houze, R. A., Jr., Squall lines observed in the vicinity of the Researcher during Phase III of GATE, in *Preprints of the 16th Radar Meteorology Conference,* pp. 206-209, American Meteorological Society, Boston, Mass., 1975.

Houze, R. A., Jr., GATE radar observations of a tropical squall line, in *Preprints of the 17th Radar Meteorology Conference,* pp. 384-389, American Meteorological Society, Boston, Mass., 1976.

Houze, R. A., Jr., Structure and dynamics of a tropical squall-line system observed during GATE, *Mon. Weather Rev., 105,* 1540-1567, 1977.

Houze, R. A., Jr., and C.-P. Cheng, Radar characteristics of tropical convection observed during GATE: Mean properties and trends over the summer season, *Mon. Weather Rev., 105,* 964-980, 1977.

Houze, R. A., Jr., and C. A. Leary, Comparison of convective mass and heat transports in tropical easterly waves computed by two methods, *J. Atmos. Sci., 33,* 424-429, 1976.

Houze, R. A., Jr., C.-P. Cheng, C. A. Leary, and J. F. Gamache, Diagnosis of cloud mass and heat fluxes from radar and synoptic data, *J. Atmos. Sci., 37,* 754-773, 1980.

Houze, R. A., Jr., S. G. Geotis, F. D. Marks, Jr., and A. K. West, Winter monsoon convection in the vicinity of North Borneo, I, Structure and time variation of the clouds and precipitation, *Mon. Weather Rev., 109,* in press, 1981.

Hoxit, L. R., C. F. Chappell, and J. M. Fritsch, Formation of mesolows or pressure troughs in advance of cumulonimbus clouds, *Mon. Weather Rev., 104,* 1419-1428, 1976.

Hudlow, M. D., Mean rainfall patterns for the three phases of GATE, *J. Appl. Meteorol., 18,* 1656-1669, 1979.

Hudlow, M. D., V. Patterson, P. Pytlowany, F. Richards, and S. Geotis, Calibration and intercomparison of the GATE C-band weather radars, *Tech. Rep. EDIS 31,* 98 pp., Natl. Oceanic and Atmos. Admin., Rockville, Md., 1980.

International Council of Scientific Unions/World Meteorological Organization (ICSU/WMO), The Planning of GARP Tropical Experiments, *GARP Rep. 4,* 78 pp., Geneva, 1970.

International Council of Scientific Unions/World Meteorological Organization (ICSU/WMO), Experimental Design Proposal for the GARP Atlantic Tropical Experiment, *GATE Rep. 1,* 188 pp., Geneva, 1972.

International Council of Scientific Unions/World Meteorological Organization (ICSU/WMO), Report on the Field Phase of the GARP Atlantic Tropical Experiment, Aircraft Mission Summary, *GATE Rep. 18,* 143 pp., Geneva, 1975.

Iwanchuk, R. M., Characteristics and distribution of precipitation areas over the tropical Atlantic, S.M. thesis, 106 pp., Mass. Inst. of Technol., Cambridge, 1973.

Johnson, R. H., The role of convective-scale precipitation downdrafts in cumulus and synoptic scale interactions, *J. Atmos. Sci., 33,* 1890-1910, 1976.

Johnson, R. H., Cumulus transports in a tropical wave composite for Phase III of GATE, *J. Atmos. Sci., 35,* 484-494, 1978.

Johnson, R. H., Cloud population properties determined by diagnostic models, in *Proceedings of the Seminar on the Impact of GATE on Large-Scale Numerical Modeling of the Atmosphere and Ocean,* pp. 109-117, National Academy of Sciences, Washington, D. C., 1980a.

Johnson, R. H., Diagnosis of convective and mesoscale motions during Phase III of GATE, *J. Atmos. Sci., 37,* 733-753, 1980b.

Kahn, P. H., and J. A. Businger, The effect of radiative flux divergence on entrainment of a saturated convective boundary layer, *Quart. J. R. Meteorol. Soc., 105,* 303-306, 1979.

Kelley, J., Summary of aircraft missions in the GATE, report, Natl. Cent. for Atmos. Res., Boulder, Colo., 1974.

Kornfeld, J., A. F. Hasler, K. J. Hanson, and V. E. Suomi, Photographic cloud climatology from ESSA III and V computer produced mosaics, *Bull. Am. Meteorol. Soc., 48,* 878-894, 1967.

Kreitzberg, C. W., and D. J. Perkey, The mechanism of convective/mesoscale interaction, *J. Atmos. Sci., 34,* 1569-1595, 1977.

Krishnamurti, T. N., H. L. Pan, C. B. Chang, J. Ploshay, D. Walker, and A. W. Oodally, Numerical weather prediction for GATE, *Quart. J. R. Meteorol. Soc., 105,* 979-1010, 1979.

Krishnamurti, T. N., Y. Ramanathan, H. L. Pan, R. J. Pasch, and J. Molinari, Cumulus parameterization and rainfall rates, I, *Mon. Weather Rev., 108,* 465-477, 1980.

Kuo, H. L., On formation and intensification of tropical cyclones through latent heat release by cumulus convection, *J. Atmos. Sci., 22,* 40-63, 1965.

Kuo, H. L., Further studies on the parameterization of the influence of cumulus convection on large-scale flow, *J. Atmos. Sci., 31,* 1232-1240, 1974.

Kuusk, A., Yu.-A. Mullamaa, H. Niilisk, T. Nilson, and M. Sulev, The structure of cloud cover in the trade-wind region on the basis of ship measurements, in *Proceedings of the International Scientific Conference on the Energetics of the Tropical Atmosphere,* pp. 155-160, International Council of Scientific Unions/World Meteorological Organization, Geneva, 1978.

Leary, C. A., Behavior of the wind field in the vicinity of a cloud cluster in the Intertropical Convergence Zone, *J. Atmos. Sci., 36,* 631-639, 1979.

Leary, C. A., Temperature and humidity profiles in mesoscale unsaturated downdrafts, *J. Atmos. Sci., 37,* 1005-1012, 1980.

Leary, C. A., and R. A. Houze, Jr., Analysis of GATE radar data for a tropical cloud cluster in an easterly wave, in *Preprints of the 17th Radar Meteorology Conference,* pp. 376-383, American Meteorological Society, Boston, Mass., 1976.

Leary, C. A., and R. A. Houze, Jr., The structure and evolution of convection in a tropical cloud cluster, *J. Atmos. Sci., 36,* 437-457, 1979a.

Leary, C. A., and R. A. Houze, Jr., Melting and evaporation of hydrometeors in precipitation from the anvil clouds of deep tropical convection, *J. Atmos. Sci., 36,* 669-679, 1979b.

Leary, C. A., and R. A. Houze, Jr., The contribution of mesoscale motions to the mass and heat fluxes of an intense tropical convective system, *J. Atmos. Sci., 37,* 784-796, 1980.

Lebedeva, N. V., and N. A. Zavelskaya, Convection conditions over the tropical ocean, paper presented at the International Conference on Scientific Results of GATE, Int. Counc. of Sci. Unions/World Meteorol. Org., Kiev, USSR, Sept. 1980.

LeMone, M. A., The structure and dynamics of horizontal roll vortices in the planetary boundary layer, *J. Atmos. Sci., 30,* 1077-1091, 1973.

LeMone, M. A., On the wind, temperature, and humidity fields in the vicinity of an east-west line of showers, *GATE Rep. 14,* vol. I, pp. 203-211, Int. Counc. of Sci. Unions/World Meteorol. Org., Geneva, 1975.

LeMone, M. A., The marine boundary layer, in *Workshop on the Planetary Boundary Layer, 14-18 August 1978, Boulder, Colorado,* pp. 182-246, American Meteorological Society, Boston, Mass., 1980.

LeMone, M. A., and W. T. Pennell, The relationship of trade wind cumulus distribution to subcloud layer fluxes and structure, *Mon. Weather Rev., 104,* 525-539, 1976.

LeMone, M. A., and E. J. Zipser, Cumulonimbus vertical velocity events in GATE, I, Diameter, intensity, and mass flux, *J. Atmos. Sci., 37,* 2444-2457, 1980.

Lilly, D. K., Models of cloud topped mixed layers under a strong inversion, *Quart. J. R. Meteorol. Soc., 94,* 292-309, 1968.

Lilly, D. K., The dynamical structure and evolution of thunderstorms and squall lines, *Annu. Rev. Earth Planet. Sci., 7,* 117-161, 1979.

Lilly, D. K., and W. Schubert, The effects of radiative cooling on a cloud-topped mixed layer, *J. Atmos. Sci., 37,* 482-487, 1980.

López, R. E., Cumulus convection and larger scale circulations, II, Cumulus and mesoscale interactions, *Mon. Weather Rev., 101,* 856-870, 1973.

López, R. E., Radar characteristics of the cloud populations of tropical disturbances in the northwest Atlantic, *Mon. Weather Rev., 104,* 268-283, 1976.

López, R. E., The lognormal distribution and cumulus cloud population, *Mon. Weather Rev., 105,* 1865-1872, 1977.

López, R. E., Internal structure and development processes of C-scale aggregates of cumulus clouds, *Mon. Weather Rev., 106,* 1488-1494, 1978.

Lord, S. J., Development and observational verification of a cumulus cloud parameterization, Ph.D. dissertation, 359 pp., Univ. of Calif., Los Angeles, 1978.

Lyne, W. M., and P. R. Rowntree, Development of a convective parameterization using GATE data, *Tech. Note 11/70,* Meteorol. Office, Bracknell, England, 1976.

Mandics, P. A., and F. F. Hall, Preliminary results from the GATE acoustic echo sounder, *Bull. Am. Meteorol. Soc., 57,* 1142–1147, 1976.

Mansfield, D. A., Squall-lines observed during GATE, *Quart. J. R. Meteorol. Soc., 103,* 569–574, 1977.

Martin, D. W., Characteristics of west African and Atlantic cloud clusters, *GATE Rep. 14,* vol. I, pp. 182–192, Int. Counc. of Sci. Unions/World Meteorol. Org., Geneva, 1975.

Martin, D. W., and O. Karst, A census of cloud systems over the tropical Pacific, Studies in Atmospheric Energetics Based on Aerospace Probings, annual report, 1968, Space Sci. and Eng. Cent., Univ. of Wisc., Madison, 1969.

Martin, D. W., and V. E. Suomi, A satellite study of cloud clusters over the tropical North Atlantic Ocean, *Bull. Am. Meteorol. Soc., 53,* 135–156, 1972.

McBride, J. L., and W. M. Gray, Mass divergence in tropical weather systems, I, Diurnal variations, *Quart. J. R. Meteorol. Soc., 106,* 501–516, 1980.

McGarry, M. M., and R. J. Reed, Diurnal variations in convective activity and precipitation during Phases II and III of GATE, *Mon. Weather Rev., 106,* 101–113, 1978.

Miller, M. J., and A. K. Betts, Traveling convective storms over Venezuela, *Mon. Weather Rev., 105,* 833–848, 1977.

Miyakoda, K., and J. Sirutis, Comparative integrations of global models with various parameterized processes of subgrid scale vertical transport: Description of the parameterization and preliminary results, *Beitr. Phys. Atmos., 50,* 445–487, 1977.

Moncrieff, M. W., and M. J. Miller, The dynamics and simulation of tropical squall lines, *Quart. J. R. Meteorol. Soc., 102,* 373–394, 1976.

Mower, R. N., G. L. Austin, A. K. Betts, C. Gautier, R. Grossman, J. Kelley, F. Marks, and D. W. Martin, A case study of GATE convective activity, *Atmos. Ocean, 17,* 46–59, 1979.

Murakami, M., Large-scale aspects of convective activity over the GATE area, *Mon. Weather Rev., 107,* 994–1013, 1979.

Nicholls, J. M., Aircraft measurements in the GARP Atlantic Tropical Experiment, *Meteorol. Mag., 108,* 349–366, 1979.

Nicholls, J. M., and M. A. LeMone, The fair weather boundary layer in GATE: The relationship of subcloud fluxes and structure to the distribution and enhancement of cumulus clouds, *J. Atmos. Sci., 37,* 2051–2067, 1980.

Nitta, T., Observational determination of cloud mass flux distribution, *J. Atmos. Sci., 32,* 73–91, 1975.

Nitta, T., Response of cumulus updraft and downdraft to GATE A/B-scale motion systems, *J. Atmos. Sci., 34,* 1163–1186, 1977.

Nitta, T., A diagnostic study of interaction of cumulus updrafts and downdrafts with large-scale motions in GATE, *J. Meteorol. Soc. Japan, 56,* 232–241, 1978.

Obasi, G. O. P., Some statistics concerning the disturbance lines of West Africa, in *Preprints of the Symposium on Tropical Meteorology,* Part II, pp. 62–66, American Meteorological Society, Boston, Mass., 1974.

Ogura, Y., and Y. L. Chen, A life history of an intense mesoscale convective storm in Oklahoma, *J. Atmos. Sci., 33,* 1458–1476, 1977.

Ogura, Y., and H.-R. Cho, Diagnostic determination of cumulus cloud populations from observed large-scale variables, *J. Atmos. Sci., 30,* 1276–1286, 1973.

Ogura, Y., and M.-T. Liou, The structure of a midlatitude squall line: A case study, *J. Atmos. Sci., 37,* 553–567, 1980.

Ogura, Y., M.-T. Liou, J. Russell, and S. T. Soong, On the formation of organized convective systems observed over the eastern Atlantic, *Mon. Weather Rev., 107,* 426–441, 1979.

Ooyama, K., A theory of parameterization of cumulus convection, *J. Meteorol. Soc. Japan, 49,* 744–756, 1971.

Ooyama, K., Objective analysis of winds over the GATE ship array (abstract), *Bull. Am. Meteorol. Soc., 61,* 1130, 1980.

Payne, S. W., and M. M. McGarry, The relationship of satellite inferred convective activity to easterly waves over west Africa and the adjacent ocean during Phase III of GATE, *Mon. Weather Rev., 105,* 413–420, 1977.

Peskov, B. E., Clouds and convection, USSR, paper presented at the International Conference on Scientific Results of GATE, Int. Counc. of Sci. Unions/World Meteorol. Org., Kiev, USSR, Sept. 1980.

Ramage, C. S., *Monsoon Meteorology,* 294 pp., Academic, New York, 1971.

Randall, D. A., Conditional instability of the first kind upside down, *J. Atmos. Sci., 37,* 125–130, 1980a.

Randall, D. A., Entrainment into a stratocumulus layer with distributed radiative cooling, *J. Atmos. Sci., 37,* 148–159, 1980b.

Raymond, D. J., A model for predicting the movement of continuously propagating convective storms, *J. Atmos. Sci., 32,* 1308–1317, 1975.

Raymond, D. J., Wave-CISK and convective mesosystems, *J. Atmos. Sci., 33,* 2392–2398, 1976.

Reed, R. J., An example of a squall line in the B-scale network, *GATE Rep. 14,* vol. 1, pp. 217–222, Int. Counc. of Sci. Unions/World Meteorol. Org., Geneva, 1975.

Reed, R. J., and E. E. Recker, Structure and properties of synoptic-scale wave disturbances in the equatorial western Pacific, *J. Atmos. Sci., 28,* 1117–1133, 1971.

Reed, R. J., D. C. Norquist, and E. E. Recker, The structure and properties of African wave disturbances as observed during Phase III of GATE, *Mon. Weather Rev., 105,* 317–333, 1977.

Reeves, R. W., C. F. Ropelewski, and M. D. Hudlow, On the relationship of the precipitation to variations in the kinematic variables during GATE, *Mon. Weather Rev., 107,* 1154–1168, 1979.

Riehl, H., Some aspects of cumulonimbus convection in relation to tropical weather systems, *Bull. Am. Meteorol. Soc., 50,* 587–595, 1969.

Riehl, H., and J. S. Malkus, On the heat balance in the equatorial trough zone, *Geophysica, 6,* 503–538, 1958.

Rodenhuis, D. R., and A. K. Betts, The convection subprogramme for GATE, *GATE Rep. 7,* 83 pp., Int. Counc. Sci. Unions/World Meteorol. Org., Geneva, 1974.

Rodenhuis, D. R., J. L. Looper, and W. M. Frank, Precipitation and cumulus transports inferred from Phase II budgets, paper presented at International Conference on Scientific Results of GATE, Kiev, USSR, Sept. 1980.

Rosenthal, S. L., Numerical simulation of tropical cyclone development with latent heat release by the resolvable scales, I, Model description and preliminary results, *J. Atmos. Sci., 35,* 258–271, 1978.

Rosenthal, S. L., The sensitivity of simulated hurricane development to cumulus parameterization details, *Mon. Weather Rev., 107,* 193–197, 1979.

Rosenthal, S. L., Numerical simulation of tropical cyclone development with latent heat release by the resolvable scales, II, Propagating small-scale features observed in the pre-hurricane phase, *Tech. Rep. ERL413-AOML29,* 43 pp., NOAA Environ. Res. Lab., Boulder, Colo., 1980.

Ruprecht, E., The vertical transport of mass, energy and water vapor by cumulus and cumulonimbus drafts within tropical disturbances, paper presented at the International Conference of Scientific Results of GATE, Int. Counc. of Sci. Unions/World Meteorol. Org., Kiev, USSR, Sept. 1980.

Sanders, F., and K. A. Emanuel, The momentum budget and temporal evolution of a mesoscale convective system, *J. Atmos. Sci., 34,* 322–330, 1977.

Sanders, F., and R. J. Paine, The structure and thermodynamics of an intense mesoscale convective storm in Oklahoma, *J. Atmos. Sci., 32,* 1563–1579, 1975.

Schubert, W. H., Experiments with Lilly's cloud-topped mixed layer model, *J. Atmos. Sci., 33,* 436–446, 1976.

Schubert, W. H., J. S. Wakefield, E. J. Steiner, and S. K. Cox, Marine stratocumulus convection, I, Governing equations and horizontally homogeneous solutions, *J. Atmos. Sci., 36,* 1286–1307, 1979a.

Schubert, W. H., J. S. Wakefield, E. J. Steiner, and S. K. Cox, Marine stratocumulus convection, II, Horizontally inhomogeneous solutions, *J. Atmos. Sci., 36,* 1308–1324, 1979b.

Semyonov, Ye. K., Some features of the intertropical convergence zone (ITCZ) from meteorological satellite observations, *Sov. Meteorol. Hydrol., 2,* 22–29, 1975.

Shapiro, L. J., The vorticity budget of a composite African tropical wave disturbance, *Mon. Weather Rev., 106,* 806–817, 1978.

Shapiro, L. J., and D. E. Stevens, Parameterization of convective effects on the momentum and vorticity budgets of synoptic-scale Atlantic tropical waves, *Mon. Weather Rev., 108,* 1816–1826, 1980.

Shupiatsky, A. B., A. I. Korotov, V. D. Menshenin, R. S. Pastushkov, and M. Jovasevic, Radar investigations of evolution of clouds in the eastern Atlantic, *GATE Rep. 14,* vol. II, pp. 177–187, Int. Counc. of Sci. Unions/World Meteorol. Org., Geneva, 1975.

Shupiatsky, A. B., A. I. Korotov, and R. S. Pastushkov, Radar investi-

gations of the evolution of clouds in the East Atlantic, in *Tropex-74*, vol. 1, *Atmosphere* (in Russian), pp. 508–514, Gidrometeoizdat, Leningrad, USSR, 1976a.

Shupiatsky, A. B., G. N. Evseonok, and A. I. Korotov, Complex investigations of clouds in the ITCZ with the help of satellite and ship radar equipment, in *Tropex-74*, vol. 1, *Atmosphere* (in Russian), pp. 515–520, Gidrometeoizdat, Leningrad, USSR, 1976b.

Sikdar, D. N., and S. J. Hentz, Kinematic structure of an Atlantic cloud cluster during GATE and its time variation, *Tellus, 32*, 439–455, 1980.

Silva Dias, M. F., Linear spectral model of tropical mesoscale systems, *Pap. No. 311*, 213 pp., Dep. of Atmos. Sci., Colo. State Univ., Fort Collins, 1979.

Simpson, J., The GATE aircraft program: A personal view, *Bull. Am. Meteorol. Soc., 57*, 27–30, 1976.

Simpson, J., and G. van Helvoirt, GATE cloud-sub cloud layer interactions examined using a three-dimensional cumulus model, *Beitr. Phys. Atmos., 53*, 106–134, 1980.

Slingo, J. M., A cloud parameterization scheme derived from GATE data for use with a numerical model, *Quart. J. R. Meteorol. Soc., 106*, 747–770, 1980.

Sommeria, G., Three-dimensional simulation of turbulent processes in an undisturbed tradewind boundary layer, *J. Atmos. Sci., 33*, 216–241, 1976.

Sommeria, G., and M. A. LeMone, Direct testing of a three-dimensional model of the planetary boundary layer against experimental data, *J. Atmos. Sci., 35*, 25–39, 1978.

Soong, S.-T., and Y. Ogura, Response of tradewind cumuli to large-scale processes, *J. Atmos. Sci., 37*, 2035–2050, 1980.

Soongo S.-T., and W.-K. Tao, Response of deep tropical cumulus clouds to mesoscale processes, *J. Atmos. Sci., 37*, 2016–2034, 1980.

Stevens, D. E., Vorticity, momentum and divergence budgets of synoptic-scale wave disturbances in the tropical eastern Atlantic, *Mon. Weather Rev., 107*, 535–550, 1979.

Stevens, D. E., R. S. Lindzen, and L. J. Shapiro, A new model of tropical waves incorporating momentum mixing by cumulus convection, *Dyn. Atmos. Oceans, 1*, 365–425, 1977.

Suchman, D., and D. W. Martin, Wind sets from SMS images: An assessment of quality for GATE, *J. Appl. Meteorol., 15*, 1265–1278, 1976.

Suchman, D., D. W. Martin, and J. Simpson, The evolving circulation of an east Atlantic cloud cluster, in *Proceedings of the 11th Technical Conference on Hurricanes and Tropical Meteorology*, pp. 333–338, American Meteorological Society, Boston, Mass., 1977.

Thompson, R. M., Jr., S. W. Payne, E. E. Recker, and R. J. Reed, Structure and properties of synoptic-scale wave disturbances in the intertropical convergence zone of the eastern Atlantic, *J. Atmos. Sci., 36*, 53–72, 1979.

Tourre, Y. M., The squall-line over West Africa and tropical eastern Atlantic Ocean during GATE, Ph.D. dissertation, 122 pp., Univ. of Va., Charlottesville, 1979.

Tschirhart, G., Les conditions aérologiques à l'avant des lignes de graines en Afrique Equatoriale, *Meteorol. Natl., 11*, 28 pp., 1958.

Warner, C., Cloud measurements on day 245 of GATE, *Atmos. Ocean, 18*, 207–226, 1980.

Warner, C., and G. L. Austin, Statistics of radar echoes on day 261 of GATE, *Mon. Weather Rev., 106*, 983–994, 1978.

Warner, C., J. Simpson, D. W. Martin, D. Suchman, F. R. Mosher, and R. F. Reinking, Shallow convection on day 261 GATE: Mesoscale arcs, *Mon. Weather Rev., 107*, 1617–1635, 1979.

Warner, C., J. Simpson, G. van Helvoirt, D. W. Martin, D. Suchman, and G. L. Austin, Deep convection on day 261 of GATE, *Mon. Weather Rev., 108*, 169–194, 1980.

Woodley, W., C. G. Griffith, J. S. Griffin, and S. C. Stromatt, The inference of GATE convective rainfall from SMS-1 images, *J. Appl. Meteorol., 19*, 388–408, 1980.

Yanai, M., S. Esbensen, and J. H. Chu, Determination of bulk properties of tropical cloud clusters from large-scale heat and moisture budgets, *J. Atmos. Sci., 30*, 611–627, 1973.

Yanai, M., J. H. Chu, T. E. Stook, and T. Nitta, Response of deep and shallow tropical maritime cumuli to large scale processes, *J. Atmos. Sci., 33*, 976–991, 1976.

Zipser, E. J., The role of organized unsaturated convective downdrafts in the structure and rapid decay of an equatorial disturbance, *J. Appl. Meteorol., 8*, 799–814, 1969.

Zipser, E. J., Mesoscale and convective-scale downdrafts as distinct components of squall-line circulation, *Mon. Weather Rev., 105*, 1568–1589, 1977.

Zipser, E. J., Kinematic and thermodynamic structure of mesoscale systems in GATE, in *Proceedings of the Seminar on the Impact of GATE on Large-Scale Numerical Modeling of the Atmosphere and Ocean*, pp. 91–99, National Academy of Sciences, Washington, D. C., 1980.

Zipser, E. J., and C. Gautier, Mesoscale events within a GATE tropical depression, *Mon. Weather Rev., 106*, 789–805, 1978.

Zipser, E. J., and M. A. LeMone, Cumulonimbus vertical velocity events in GATE, II, Synthesis and model core structure, *J. Atmos. Sci., 37*, 2458–2469, 1980.

Zipser, E. J., R. J. Meitin, and M. A. LeMone, Mesoscale motion fields in association with a slow-moving GATE convective band, *J. Atmos. Sci., 38*, in press, 1981.